fire

MDPI

Article

Fire-Induced Alterations of Soil Properties in Albic Podzols Developed under Pine Forests (Middle Taiga, Krasnoyarsky Kray)

Alexey A. Dymov [1,2,*], Viktor V. Startsev [1], Evgenia V. Yakovleva [1], Yurii A. Dubrovskiy [1], Evgenii Yu. Milanovsky [3], Dariy A. Severgina [1], Alexey V. Panov [4] and Anatoly S. Prokushkin [4]

1 Institute of Biology Komi Scientific Center Ural Branch of Russian Academy of Science, Kommunisticheskaya 28, 167982 Syktyvkar, Russia
2 Department of Physics and Soil Reclamation, Faculty of Soil Science, Lomonosov Moscow State University, 119991 Moscow, Russia
3 Institute of Physicochemical and Biological Problems in Soil Science, RAS, Institutskaya Str., 2/2, 142290 Pushchino, Russia
4 V. N. Sukachev Institute of Forest SB RAS, Akademgorodok 50/28, 660036 Krasnoyarsk, Russia
* Correspondence: dymov@ib.komisc.ru or aadymov@gmail.com; Tel.: +7-495-939-42-07 or +7-8212-24-51-15

Abstract: Fires are one of the most widespread factors of changes in the ecosystems of boreal forests. The paper presents the results of a study of the morphological and physicochemical properties and soil organic matter (SOM) of Albic Podzols under pine forests (*Pinus sylvestris* L.) of the middle taiga zone of Siberia (Krasnoyrsky kray) with various time passed after a surface fire (from 1 to 121 years ago). The influence of forest fires in the early years on the chemical properties of Albic Podzols includes a decrease in acidity, a decrease in the content of water-soluble compounds of carbon and nitrogen and an increase in the content of light polycyclic aromatic hydrocarbons (PAHs) in organic and upper mineral horizons. Podzols of pine forests that were affected by fires more than forty-five years ago are close to manure forest soils according to most physical and chemical properties. Significant correlations were found between the thickness ($r = 0.75$, $p < 0.05$), the moisture content ($r = 0.90$, $p < 0.05$) of organic horizons and the content of ∑PAHs in the organic horizon ($r = -0.71$, $p < 0.05$) with the time elapsed after the fire (i.e., from 1 to 121 years). The index of the age of pyrogenic activity (IPA) calculated as the ratio of ∑ PAHs content in the organic horizon to ∑ PAHs at the upper mineral horizon is significantly higher in forests affected by fires from 1 to 23 years than for plots with «older» fires (45–121 years). Thus, the article presents the conserved and most changing factors under the impact of fires in the boreal forests of Russia.

Keywords: boreal forest; wildfire; C; N; stable isotopes; PAHs

Citation: Dymov, A.A.; Startsev, V.V.; Yakovleva, E.V.; Dubrovskiy, Y.A.; Milanovsky, E.Y.; Severgina, D.A.; Panov, A.V.; Prokushkin, A.S. Fire-Induced Alterations of Soil Properties in Albic Podzols Developed under Pine Forests (Middle Taiga, Krasnoyarsky Kray). *Fire* **2023**, *6*, 67. https://doi.org/10.3390/fire6020067

Academic Editor: Grant Williamson

Received: 30 December 2022
Revised: 1 February 2023
Accepted: 8 February 2023
Published: 13 February 2023

1. Introduction

Fires are one of the most important disturbance factors affecting Pine forests and development of Podzols during Holocene [1–3]. Fires in boreal forests, particularly in pine forests, are a natural historical factor in their development [4–6]. The pine lichen forests growing on soils with sandy and sandy loam textures are most affected by fires [7–10]. The light texture of the bed rocks leads to well-drained soils and organic horizons drying out, and provides the highest flammability [11]. Repeated forest fires are a significant factor for the co-existence of both Pine forests and Albic Podzols [12,13]. According to Soil Taxonomy [14], this soil is classified as Spodosols which refers to the red, brown or black (Bs) horizon below the light colored near-surface layer. Under acidic conditions, aluminum, iron and organic compounds migrate from the bleached eluvial horizon (E) down to the Bs horizon with percolating rainwater [15]. The spodic horizon (Bs) has high concentration amorphous mixtures of organic matter and aluminum, with or without iron, which have accumulated. Podzols are found only in coarse-textured and base-poor parent materials—most often sands and sandy tills [16]. Significant areas of Podzols are

represented in the boreal forest regions. Podzols cover about 485 million ha worldwide, mainly in the temperate and boreal regions of the Northern Hemisphere [17]. In the Krasnoyrsky kray, Podzols cover 3.7% (86 tsh. km^2) of territory [18].

Fires can affect morphological and physicochemical properties of soil [10,11,19], that persist for several thousands of years [20]. In the soils of recently burnt areas, a decrease in acidity [7] and an increase in ash elements affecting the exchange properties of soils were noted [21]. Wildfires in the boreal forest can affect SOM, including its resistance to decomposition [22,23]. In the short-term, large quantities of SOM C are released into the atmosphere when the vegetation biomass and SOM on the soil surface are combusted.

The pyrogenically altered carbon compounds can be stable and play a significant role in the global carbon cycle [24–26]. Santin et al. [27] showed that soils contain a significant concentration of pyrogenic carbon (PyC). Some of the organic compounds formed during the cyclization of polymer molecules can be sufficiently resistant to decomposition [26,28,29]. Fires can change the carbon and nitrogen isotopic composition [30]. Yet, data on the long-term effect of pyrogenesis on the isotopic composition of carbon and nitrogen have not been found in the literature. Polycyclic aromatic hydrocarbons (PAHs) and benzene polycarboxylic acids (BPCAs) are often used as fire biomarkers in soil organic matter [31–35]. According to Rey-Salgueiro et al. [36], the greatest PAH concentrations are formed at temperatures up to 600 ºC. PAHs are usually formed under biomass combustion with high lignin content [37]. PAHs are known to have cancerogenic, mutagenic and toxic properties [38] and are also often used for estimating pyrogenic impact on soil organic matter due to their aromatic structure [35]. The forests of Siberia are most susceptible to fires in the boreal zone of Eurasia, but assessments of changes in the properties of soils in this region are extremely rare [39].

The aim of the work is to assess changes in Albic Podzols of the middle taiga of Siberia under the influence of surface fires and during post-fire succession.

2. Materials and Methods

2.1. Area Description, Soil Sampling, Geobotanical Descriptions and Fire Event-Dating

The study area is located in the middle taiga subzone nearby the ZOTTO International Observatory (60°26′ N, 89°24′ E) (Figure 1). The mean annual air temperature in the Zotino region (Krasnoyrsky kray) according to the Bor weather station is −3.5 °C. The sum of temperatures above 10 °C varies from 1200 to 1400 °C. The annual rainfall is 594 mm.

In this study, in the summer period of 2019, we have selected five lichen pine forests affected by fires from 1 to 121 years ago. Photos of landscapes and soil profiles are presented on Figure S1. In each site, we have conducted vegetation descriptions (reveles) on 20 m × 20 m square plots using the standard geobotanical methods [40]. Undergrowth, herb-dwarf shrub and moss-lichen strata were characterized by the relative abundance of species and the total projective cover (TPC) of each. Latin names are given according to http://www.worldfloraonline.org/ (access date 25 December 2022).

Soil profiles were investigated in each square plot up to the 100–120 cm depth. Two more random soil profiles of up to 40 cm depths were excavated in the center of round inventory plots. Soil samples were taken from each genetic horizon. Organic layers were collected in triplicate from a 20 cm × 20 cm area. Mineral soil samples for chemical analyses were collected from five points from the pit and then the samples were mixed. The field diagnostics were performed according to the World Reference Base for Soil Resources [17]. The color of the horizons was determined according to the Munsell soil color chart [41]. We added «pyr» to the horizon name when, during the field description, inclusions associated with fires were diagnosed (coal, soot, etc.).

The tree-ring core samples from three to five cuts' cross-sections for estimation fire scars were obtained according to [42–44].

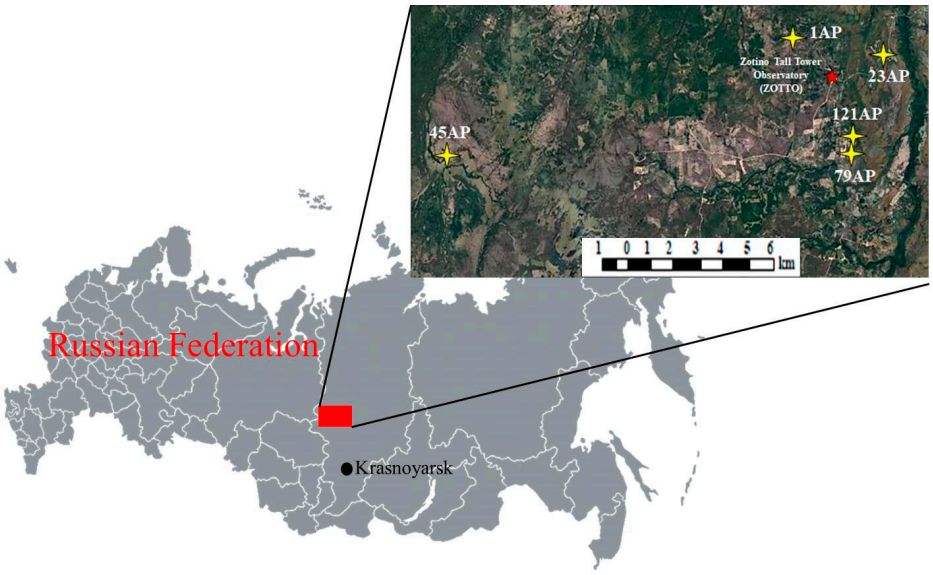

Figure 1. Location of study sites (the scheme is based on http://www.glovis.usgs.gov, accessed on 30 December 2022).

2.2. General Soil Analysis

Soil samples were air-dried under root temperature and sieved through a sieve with a mesh size of 2 mm. Pyrogenic and organic samples were crushed with a laboratory grinder. Chemical analyses of the soils were performed according to classical methods [45]. The methods of classical analyses are described in detail in our earlier works [10,35]. Specific surface area (SSA) was determined on a surface area analyzer (Sorbtometr-M, Katakon, Russia) with N_2 as the adsorbate gas at the Faculty of Soil Science, Lomonosov Moscow State University (Moscow, Russia). The method was described in detail previously [35].

2.3. Soil Organic Matter and PAHs Analysis

$C_{tot.}$ and $N_{tot.}$ were determined by dry combustion on an EA-1100 analyzer (Carlo Erba, Milano, Italy). Densiometric fractionation was performed with a sodium polytungstate (SPT0) solution with a density of 1.60 ± 0.03 g cm^{-3} according to the method proposed [46] with recommendations [47].

The stable isotope ratios $^{13}C/^{12}C$ and $^{15}N/^{14}N$ were determined by an IsoPrime 100 isotope ratio mass-spectrometer (IsoPrime Corporation, Cheadle, UK) and vario ISOTOPE cube elemental analyzer (Elementar Analysen systeme GmbH, Hanau, Germany).

Water-soluble organic carbon (WSOC) and nitrogen (WSON) were analyzed according to the previously described method [12]. The extraction of PAHs from the soils was made on an Accelerated Solvent Extractor 350 (Thermo Scientific™, Waltham, MA, USA) in the Chromatography Collective Use Center of the IB FRC Komi SC UrB RAS. The method was described in detail previously [2].

2.4. Statistics

Significance differences and correlation coefficients were calculated using the STATISTICA 10.0 (Stat. Soft Inc., Tusla, OK, USA) software. Differences were considered significant at the significance level $p < 0.05$.

3. Results

3.1. Vegetation at the Study Sites

All study sites represent postfire development stages of Scots pine forests dominated in ground cover vegetation by ericoids *Vaccinium vitis-idaea*, *Ledum palustre* and lichens *Cladonia arbuscular*, *C. rangiferina* and *C. crispata*. The plant communities have similar species

composition and structure, and belong to the association Pinetum vaccinioso-cladinosum (Table 1).

Table 1. Total projective cover (TCP) and dominant species of lower layers of plant communities of Pinetumvaccinioso-cladinosum formed on Albic Podzols.

Age from Last Fire, Years	Total Projective Cover (TCP) and Dominant Species of Lower Vegetation Layers
1	Dwarf-shrub herb layer 3%, *Vaccinium vitis-idaea*, *Calamagrostis* sp., *Chamaenerion angustifolium* Moss-lichen layer single burned residues of lichens
23	Dwarf-shrub herb layer 5%, *Vaccinium vitis-idaea*, *Calamagrostis obtusata* Moss-lichen layer 50%, *Cladonia arbuscula*, *Cladonia rangiferina*, *Cladonia crispata*, *Cladonia cornuta*
45	Dwarf-shrub herb layer 30%, Vaccinium vitis-idaea, Ledum palustre, *Vaccinium uliginosum* Moss-lichen layer 90%, *Cladonia arbuscula*, *Cladonia rangiferina*, *Cladonia crispata*, *Pleurozium schreberi*
79	Dwarf-shrub herb layer 25%, *Vaccinium vitis-idaea*. *Calamagrostis obtusata*, *Diphasium complanatum*, *Vaccinium myrtillus* Moss-lichen layer 80%, *Cladonia arbuscula*, *Cladonia rangiferina*, *Cladonia crispata*, *Pleurozium schreberi*
121	Dwarf-shrub herb layer 5%, *Vaccinium myrtillus*, *Vaccinium vitis-idaea*, *Ledum palustre*, *Diphasium complanatum*, *Empetrum hermaphroditum* Moss-lichen layer 90%, *Cladonia arbuscula*, *Cladonia rangiferina*

Only single vascular plants occurred at the study plots at the initial stage of post-fire restoration (1 year after a fire, 1AP). Then, during the post-fire succession, the TPC of herb-dwarf shrub layer increases, reaching 20–30% at the plots burned 45–79 years ago (45AP and 79AP). However, the TCP of the herb-dwarf shrub layer on the 121AP plot decreases to only 5%.

However, the TCP of the herb-dwarf shrub layer on the 121AP plot decreases to only 5%. In the moss-lichen cover, there were no living mosses and lichens at the plot 1AP due to high intensive burning (fire scars on pine tree trunks are up to 10–12 m high). At the plot burned 23 years ago, total projective cover of the moss-lichen layer already reached 50% and further increased up to 80–90% at the plots burned out 45–121 years ago. The species diversity of vascular plants, mosses and lichens increased during the post-fire succession from 1–2 species at the 1AP to 8–9 species per plot at the later stages (Table 1).

3.2. Morphological Properties of Soils

The Albic Podzols surveyed in the studied fire chronosequence (from 1 to 121 year old) have the typical morphology for medium to high developed soils on well-drained coarse textured sands. Soil profiles have the following vertical structure: Oi/Q_{pyr}—Oe, $_{pyr}$—E_{pyr}—E—Bs—B. In mature pine forests (45–121AP), the soil organic horizon (5.7 ± 1.2 to 9.7 ± 0.6 cm thickness) consists of several subhorizons composed of by plant debris with different stages of decomposition. The upper subhorizon Oi (1 to 3 cm deep) appeared already in the early stage of post fire succession (23AP) and consists of poorly decomposed remnants of ground vegetation and trees. The bottom Oe, $_{pyr}$ subhorizon in all studied plots contains plant residues at an average degree of decomposition with usually high values of charcoal particles of different sizes. A light gray-brownish (10YR4/1-10YR6/1) sandy horizon E_{pyr} is formed below the organic horizon with a capacity of 4 to 6 cm and is enriched with dark colored organic matter and charcoal. The whitish, light gray (7.5YR8/1-10YR8/1) horizon E (6 to 29 cm thickness) that appeared below does not have visible structures and irregularly contain charcoal particles. The spodic horizon Bs (10 to

40 cm thickness) is yellowish brown (7.5YR6/8-10YR6/8), sandy, unstructured and is characterized by the accumulation of SOM forming complex compounds with Al and Fe. The deepest B horizon is non-uniform in color (from 2.5.6/6-2.5Y7/4 to 10YR 4/6) and is also without structures, but in the same case, this horizon can be more heavy-textured. Clay-like material underlaid the sandy B horizon at site 45AP.

The moisture content and thickness of the organic horizons are important characteristics of the fire's effect (Figure 2a). The thickness of the organic horizon Q_{pyr} in the area affected by fire a year ago (1AP) was minimal due to complete or partial combustion of lichen and organic layers, and was presented by charred organic material. Along with post-fire recovery of ground vegetation and the pine canopy, the thickness of the organic horizons gradually increased with age because of the fire impact, due to the accumulation of decay of ground cover plants and trees. The largest values of the thickness of the entire organic horizon were measured for the soil of the oldest site 121AP (8.3 ± 2.9 cm).

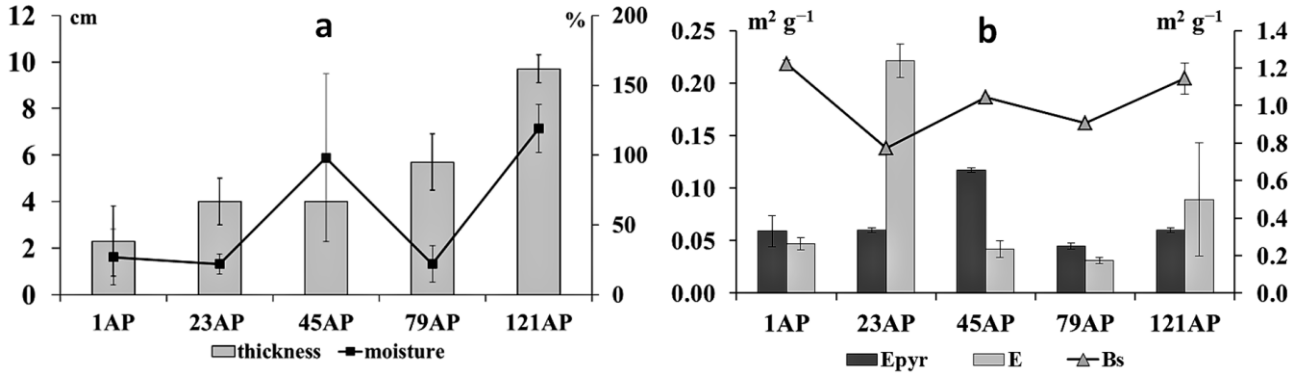

Figure 2. The thickness (left axis) and moisture content (right axis) of the organic horizons in the study soils (**a**). Specific surface area (**b**) of upper horizons' studied soils. E and E_{pyr} on the left axis; organic layer and Bs on the right axis.

The lowest moisture content was found in the 1AP (WSC = 27%) and 23AP (22%) plots, 1 and 23 years after the fire, respectively (Figure 2a). Surprisingly low soil moisture content (22%) was also found at the 79 AP site. The highest WSC (119 ± 17%) was found in organic horizons of the oldest forest affected by a fire 121 years ago.

The correlation analysis for the Q_{pyr} (Oe) pyrogenic horizon showed a significant positive relationship between the thickness ($r = 0.75$, $p < 0.05$) and the moisture content of the horizon ($r = 0.90$, $p < 0.05$) with the time elapsed after the fire (i.e., from 1 to 121 years).

3.3. The Main Chemical Soil Properties

The investigated Podzols have typical chemical properties (Table 2). The soil horizons vary from slightly (pH_{H2O} 6.1) to strongly acidic (pH_{H2O} 4.1). The lowest pH_{H2O} was observed in organic horizons, where the pH_{H2O} values varied from 4.1 to 5.6. The highest pH_{H2O} (5.6) was observed in the Q layer (charred organic material) of the 1AP site. Surprisingly, the most acidic condition among analyzed soils was the organic layer from the 23AP site (pH_{H2O} 4.1). Organic layer Oi and Oe subhorizons in the oldest 121AP site have a pH_{H2O} of 4.4 and 4.2, respectively. Those are characterized as the lowest pH_{KCl}. Intermediate stages of post-fire restoration demonstrated a relatively narrow variation range of pH_{H2O} values between 4.6 and 4.8.

Table 2. Chemical parameters of the studied soils.

Site	Horizon	Depth, cm	pH		$C_{tot.}$	$N_{tot.}$	C/N	WSOC	WSON	Ca^{2+}	Mg^{2+}	K^+	Na^+	∑	BS, %	CEC
			H_2O	KCl	g kg^{-1}			mg g^{-1}		mmol 100 g^{-1}						
	Q_{pyr}	0–1	5.6	4.1	448 ± 16	19.4 ± 2.1	27	0.46 ± 0.09	0.04 ± 0.01	10.26	0.828	1.393	0.057	12.54	23	54.0
	E_{pyr}	1–6	4.7	3.4	34 ± 5	0.93 ± 0.19	43	0.05 ± 0.01	0.005 ± 0.001	0.17	0.009	0.033	0.005	0.22	8	2.8
	E	6–17	5.8	4.7	2.7 ± 0.6	0.25 ± 0.07	13	0.03 ± 0.01	0.004 ± 0.001	–	–	0.001	–	–	1	0.2
1AP	Bs1	17–30	5.5	5.0	7.9 ± 1.8	0.50 ± 0.10	18	0.022 ± 0.004	0.003 ± 0.001	–	–	0.011	–	0.01	1	1.0
	Bs2	30–50	5.8	4.9	3.0 ± 0.7	0.32 ± 0.09	11	0.020 ± 0.004	0.008 ± 0.002	–	–	0.016	0.004	0.04	–	–
	B1	50–80	5.5	4.5	1.6 ± 0.4	0.18 ± 0.05	10	0.016 ± 0.003	0.005 ± 0.001	0.03	–	0.017	0.006	0.06	5	1.2
	B2	80–100	5.8	4.8	1.21 ± 0.28	0.12 ± 0.04	12	0.025 ± 0.005	0.005 ± 0.001	0.08	–	0.015	0.003	0.10	29	0.3
	Oi	0–1	4.7	3.6	444 ± 16	12.9 ± 1.4	40	5.57 ± 1.11	0.19 ± 0.04	10.23	1.542	2.314	0.051	14.14	22	63.3
	$Oe_{,pyr}$	1–3	4.1	3.1	375 ± 13	11.7 ± 1.3	37	1.57 ± 0.31	0.07 ± 0.01	4.14	0.430	0.997	0.062	5.63	9	64.3
	E_{pyr}	3–8	4.2	3.3	29 ± 4	0.95 ± 0.19	36	0.10 ± 0.02	0.004 ± 0.001	0.08	0.022	0.027	0.010	0.14	4	3.3
23AP	E	8–14	4.7	3.9	5.3 ± 1.2	0.23 ± 0.07	27	0.05 ± 0.01	–	0.01	0.005	0.004	–	0.02	2	1.2
	Bs	14–30	5.4	4.8	9.7 ± 2.2	0.51 ± 0.10	22	0.04 ± 0.01	–	0.01	0.009	0.017	0.003	0.04	3	1.3
	B1	30–75	5.5	5.2	2.3 ± 0.5	0.18 ± 0.05	15	0.025 ± 0.005	–	0.03	0.011	0.018	0.004	0.06	8	0.8
	B2	75–120	6.1	5.0	–	–	–	0.019 ± 0.004	–	0.09	0.018	0.017	0.006	0.13	13	1.0
	Oi	0–3	4.6	3.6	439 ± 15	9.3 ± 1.0	55	5.75 ± 1.15	0.26 ± 0.05	6.28	1.352	2.487	0.194	10.32	27	38.6
	Oe, pyr	3–5	4.6	3.3	357 ± 12	9.2 ± 1.0	45	1.48 ± 0.30	0.07 ± 0.01	1.17	0.215	0.434	0.120	1.94	9	22.7
	E_{pyr}	5–11	4.8	3.9	27 ± 4	0.78 ± 0.16	40	0.08 ± 0.02	0.003 ± 0.001	0.03	–	0.040	0.020	0.09	5	1.8
45AP	E	11–20	5.6	4.2	2.5 ± 0.6	0.17 ± 0.05	17	0.03 ± 0.01	0.003 ± 0.001	0.03	–	0.023	0.021	0.07	31	0.2
	Bs	20–45 (50)	5.7	4.8	5.2 ± 1.2	0.34 ± 0.10	18	0.020 ± 0.004	–	0.08	–	0.030	0.021	0.13	22	0.6
	B1	45 (50)–70	6.0	4.9	2.3 ± 0.5	0.19 ± 0.06	14	0.015 ± 0.003	–	0.02	–	0.018	0.016	0.05	–	–
	B2	70–90	5.8	4.0	1.8 ± 0.4	0.22 ± 0.06	10	0.04 ± 0.01	0.003 ± 0.001	3.53	2.080	0.219	0.097	5.92	54	10.9
	B3	90–110	5.9	4.0	1.6 ± 0.4	0.16 ± 0.05	12	0.03 ± 0.01	0.004 ± 0.001	3.92	2.270	0.188	0.101	6.48	67	9.7
	Oi	0–1	4.8	3.6	395 ± 14	10.4 ± 1.1	44	4.64 ± 0.93	0.19 ± 0.04	9.75	1.128	1.883	0.033	12.80	34	38.2
	Oe	1–2	4.6	3.6	443 ± 16	10.1 ± 1.1	51	3.16 ± 0.63	0.17 ± 0.03	8.99	0.944	2.331	0.065	12.32	33	37.4
	E_{pyr}	2–6	4.7	3.5	32 ± 5	1.01 ± 0.20	37	0.08 ± 0.02	0.004 ± 0.001	0.15	0.032	0.023	0.005	0.21	13	1.6
79AP	E	6–16	5.0	3.9	6.2 ± 1.4	0.41 ± 0.08	18	0.038 ± 0.008	0.003 ± 0.001	0.02	0.013	0.009	0.002	0.04	–	–
	Bs	16–35	5.4	4.6	7.4 ± 1.7	0.45 ± 0.09	19	0.053 ± 0.011	–	0.04	0.027	0.021	0.016	0.10	9	1.1
	B1	35–60	5.9	4.7	2.6 ± 0.6	0.19 ± 0.06	16	0.057 ± 0.011	0.004 ± 0.001	0.09	0.042	0.019	0.014	0.17	17	1.0
	B2	60–90	5.9	4.7	1.4 ± 0.3	0.13 ± 0.04	13	0.020 ± 0.004	–	0.23	0.079	0.026	0.009	0.34	33	1.0
	Oi	0–2	4.4	3.2	460 ± 16	11.2 ± 1.2	48	2.28 ± 0.46	0.15 ± 0.03	6.93	1.091	2.045	0.054	10.12	24	41.8
	Oe, pyr	2–4	4.3	3.0	442 ± 16	8.9 ± 1.0	58	1.34 ± 0.27	0.09 ± 0.02	4.10	0.507	0.613	0.040	5.26	11	48.0
	E_{pyr}	4–10	4.9	3.3	11.8 ± 2.7	0.42 ± 0.08	33	0.12 ± 0.02	0.006 ± 0.001	0.10	0.011	0.030	0.006	0.15	10	1.4
121AP	E	10–20	5.1	3.8	3.1 ± 0.7	0.28 ± 0.08	13	0.040 ± 0.008	0.004 ± 0.001	0.03	–	0.005	0.001	0.04	17	0.2
	Bs1	20–40	5.5	4.7	5.3 ± 1.2	0.32 ± 0.09	21	0.035 ± 0.007	0.004 ± 0.001	0.02	0.001	0.028	0.007	0.06	5	3.1
	Bs2	40–60	5.6	4.6	2.6 ± 0.6	0.22 ± 0.06	19	0.022 ± 0.004	0.003 ± 0.001	0.04	0.007	0.027	0.005	0.08	7	1.3
	B	60–100	5.7	4.5	<1.0	<0.1	14	0.031 ± 0.006	0.007 ± 0.001	0.06	0.005	0.017	0.006	0.09	22	1.2

Note: ∑—is the sum of the exchange cations, BS—base saturation, CEC—cation exchange capacity, WSOC—water soluble organic carbon, WSON—water soluble organic nitrogen, dash—below the definition limit. B3 horizons contained, comparable to organic layers, levels of exchangeable cations (up to 6.5 mmol 100 g^{-1} of the soil). Eluvial horizons (E and E_{pyr}) demonstrated the least sum of exchangeable cations.

The pH_{H2O} values of soil mineral horizons ranged from 4.7 to 6.1. There is the common tendency of decreasing soil acidity with the soil depth in all soil profiles, as the pH values increase from 4.2–4.9 in the upper mineral horizons (E_{pyr} and E) to 5.7–6.1 in the deepest horizons (Bs and B). A fire impact on soil acidity at upper mineral horizons (E_{pyr} and E) is not recognized even one year after the fire (1AP site). Despite the low total projective cover (TPC) of ground vegetation, an early restoration stage of post-fire succession (23AP site) is characterized by a rather strong acidification of both E_{pyr} and E horizons (pH 4.2 and 4.7, respectively).

The studied soils have similar soil texture and a weak profile differentiation of texture fraction contents. The upper soil horizon presented by sandy and loamy sands deposits are underlain by silty clay and clay loam deposits. The increasing clay content up to 19–24% from 70 cm was revealed only for the 45AP site. The upper coarse-textured horizons are characterized by a high sandy fraction and vary from 85 to 98%; the content of the clay fraction was 0–4%; low content of the silty fraction (1–6%) was detected. There was no distinct pyrogenic effect on the texture of upper mineral horizons.

The organic horizons are characterized by the highest sum of exchangeable cations, varying from 10 to 14 mmol 100 g^{-1} of the soil in upper Oi horizons and from 1.9 to 12.2 in $Oe_{,pyr}$ (Table 2). The content of exchangeable cations decreased 10–100-fold in the mineral soil horizons (0.02–0.17 mmol 100 g^{-1} of the soil), except the 45AP site where there was clayey B2.

Calcium cations generally predominate among the exchangeable bases (60 ± 15%, up to 82%). The highest variation of exchangeable Ca^{2+} concentrations observed for the 1AP

site: from 0 in E, and Bs1 and Bs2 horizons to 10.3 mmol 100 g^{-1} found in the pyrogenic Q_{pyr} horizon. The exchangeable Mg^{2+} content ranges among soils from 0.0 to 2.3 mmol 100 g^{-1} of the soil (15 ± 10%). The exchangeable K^+ can be the only base detected in soils such as in the E and Bs1 horizons of the 1AP site and varies from 0.001 to 2.5 mmol 100 g^{-1} (24 ± 17%). Sodium in general has the least content (7 ± 8%) among bases varying from 0 to 0.19 mmol 100 g^{-1}, and only for the 45AP site, its contribution to the sum bases reaches 32% in the Bs horizon. The base saturation is uneven throughout the soil profiles in all studied plots and varies from 0 to 67%.

Specific surface area (SSA) was very different among the soil horizons and studying soils (Figure 2b). The highest values were observed in organic (0.224–0.618 m^2 g^{-1}) and spodic illuvial Bs horizons (0.772–1.221 m^2 g^{-1}). Among the organic horizons, the Q_{pyr} horizon at the site 1AP demonstrated the highest SSA (0.586 ± 0.021 m^2 g^{-1}). The SSA in the organic horizons of the rest sites (23–121 years after the fire) ranged from 0.224 ± 0.006 to 0.429 ± 0.008 m^2 g^{-1} with a decrease in SSA with time elapsed after a fire. Among the mineral horizons, the lowest values were found in the eluvial E_{pyr} (0.045–0.117 m^2 g^{-1}) and E horizons (0.031–0.221 m^2 g^{-1}).

The SSA has strong correlation values with the content of exchangeable Ca^{2+} (r = 0.99, $p < 0.05$), Mg^{2+} (r = 0.99, $p < 0.05$), K^+ (r = 0.98, $p < 0.05$), Na^+ (r = 0.96, $p < 0.05$), their sum (r = 0.99, $p < 0.05$) and CEC (r = 0.94, $p < 0.05$). In addition, the soil texture demonstrated a strong influence on SSA in mineral soil; the SSA has correlation with silt and clay contents (r = 0.98, $p < 0.05$).

3.4. Carbon and Nitrogen Content, Water Soluble Organic Matter

Carbon and nitrogen concentrations in the studied Podzols vary from 1.0 to 460 g kg^{-1} and from 0.1 to 19.4 g kg^{-1}, respectively (Table 2). There is the common pattern in the distribution of the SOC (Figure 3a), C:N ratio (Figure 3b) and stable isotopes of C and N (Figure 3c,d) throughout the Podzol soil profile as shown for diverse sites 1 and 121.

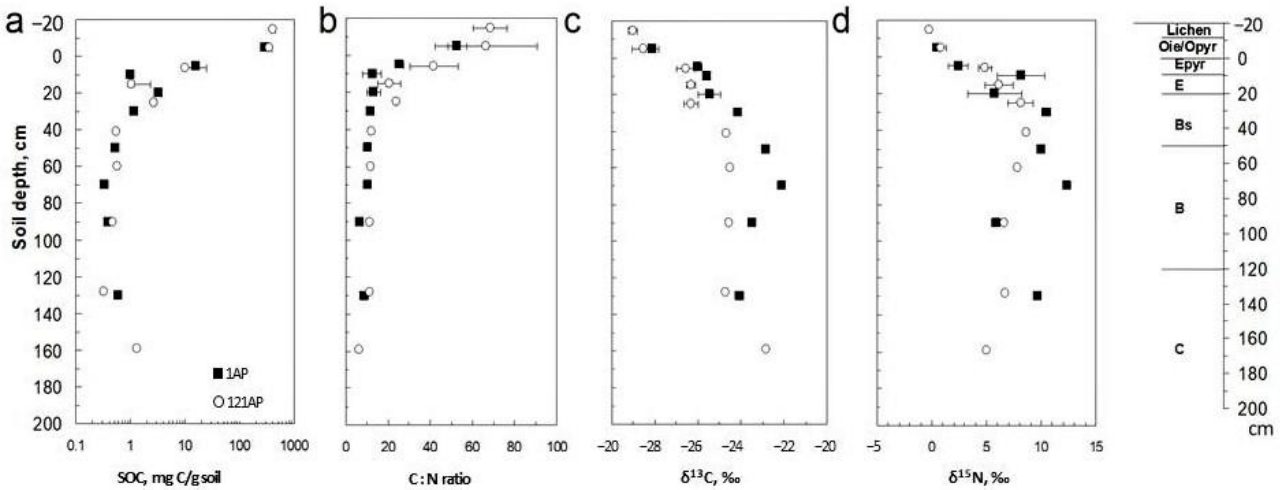

Figure 3. Changes of SOC content (**a**), C:N ratio (**b**), δ^{13}C-SOC (**c**) and δ^{15}N (**d**) with soil depth in pine forests affected by wildfires 1 and 121 years ago.

The largest concentrations of both $C_{tot.}$ and $N_{tot.}$ appear in soil organic horizons and they decrease 10-fold below in the upper mineral E_{pyr} horizon. Nevertheless, there is an indication of increased carbon (11.8–34 g kg^{-1}) and nitrogen (0.4–1.1 g kg^{-1}) content in these pyrogenic horizons (E_{pyr}). Soils of all study plots demonstrated considerable depletion of eluvial E horizons with SOM (both $C_{tot.}$ and $N_{tot.}$) and its accumulation below in an illuvial spodic Bs horizon. In deeper subsoil horizons, the content of both $C_{tot.}$ and $N_{tot.}$ remain relatively constant at levels of 0.5 ± 0.1 and 0.05 ± 0.2 g kg^{-1} of soil, respectively. Similarly, the C:N ratio decreases from 66 ± 24 in the organic layers to 20 ± 2

in the Bs horizon and further to 13 ± 2 in the deeper B horizons (Figure 3b). The C:N ratio decreased in the Q_{pyr} horizon (1AP) after a fire ($p < 0.05$).

The upper soil horizons (E_{pyr} and E) were divided into three fractions using a heavy liquid (fPOM $_{< 1.6}$, oPOM $_{< 1.6}$, MaOM $_{> 1.6}$). MaOM $_{> 1.6}$ fractions predominate in the studied horizons (Table 3). Its content varied from 91.91 to 98.45% in pyrogenic horizons E_{pyr} and 98.53–99.76% in E horizons. The content of light fractions did not exceed 4%. Pyrogenic horizons E_{pyr} contained from 0.73 to 5.44% of fractions fPOM $_{<1.6}$ and from 0.25 to 3.98% of fractions oPOM $_{<1.6}$. The content of the fPOM $_{<1.6}$ in the E horizons was 0.11–0.49%, and the oPOM $_{< 1.6}$ varied from 0.06 to 0.73%. It is established that the pyrogenic horizons E_{pyr} contained, in general, 2–29 times more fractions, fPOM $_{< 1.6}$, and 1–66 times more fractions, oPOM $_{< 1.6}$, than the horizon E. Despite the smaller amount, the main carbon pool is contained in fPOM $_{< 1.6}$ and oPOM $_{< 1.6}$ fractions. The carbon content in the fPOM $_{< 1.6}$ varied from 44 ± 7 to 379 ± 13 g kg^{-1}; in the oPOM$_{< 1.6}$ carbon content varied from 15 ± 3 to 512 ± 18. The content of nitrogen in the densimetric fractions is significantly lower than that of carbon. Fractions fPOM < 1.6 contained 1.6 ± 0.3 to 8.2 ± 0.9 g kg^{-1}. The oPOM$_{< 1.6}$ fractions contained 0.91–10.5 g kg^{-1}. Fraction MaOM $_{> 1.6}$ contained 1.0–6.70 g kg^{-1} carbon and 0.1–0.26 g kg^{-1} nitrogen.

Table 3. Contribution of the fraction; carbon and nitrogen content in densimetric fractions of E_{pyr} and E horizons.

Site, Horizons		fPOM $_{< 1.6}$				oPOM $_{< 1.6}$				MaOM $_{> 1.6}$			
		Mass, %	C	N	C/N	Mass, %	C	N	C/N	Mass, %	C	N	C/N
			g kg^{-1}				g kg^{-1}				g kg^{-1}		
1AP	E_{pyr}	2.16	358 ± 13	7.5 ± 0.8	56	0.54	350 ± 12	9.7 ± 1.1	42	97.74	1.40 ± 0.03	0.1	16
	E	0.49	44 ± 7	1.6 ± 0.3	32	0.42	15 ± 3	0.91 ± 0.18	19	99.07	1.0	0.1	12
23AP	E_{pyr}	3.75	319 ± 11	6.4 ± 0.7	58	0.25	512 ± 18	10.2 ± 1.1	59	94.44	1.0	0.1	12
	E	0.35	293 ± 29	5.1 ± 1.0	67	0.08	208 ± 21	4 ± 0.8	61	98.82	1.250 ± 0.029	0.1	15
45AP	E_{pyr}	1.30	379 ± 13	5.8 ± 1.2	76	1.06	45 ± 7	1.8 ± 0.4	29	97.20	1.60 ± 0.04	0.1	19
	E	0.48	42 ± 6	1.23 ± 0.25	40	0.39	16 ± 4	1.38 ± 0.28	14	99.41	1.0	0.1	12
79AP	E_{pyr}	0.73	363 ± 13	8.3 ± 0.9	51	0.52	385 ± 14	9.8 ± 1.1	46	98.45	1.60 ± 0.04	0.1	19
	E	0.4	154 ± 15	4.1 ± 0.8	44	0.73	30 ± 4	1.7 ± 0.3	21	98.53	1.0	0.1	12
121AP	E_{pyr}	2.17	278 ± 28	5.6 ± 1.1	58	0.54	103 ± 10	4 ± 0.8	30	97.99	1.0	0.1	12
	E	0.45	154 ± 15	3.8 ± 0.8	47	0.08	29 ± 4	1.6 ± 0.3	21	99.75	1.0	0.1	12

The stable isotope ratios of carbon ($\delta^{13}C$) and nitrogen ($\delta^{15}N$) of bulk soil demonstrated the enrichment by heavy isotopes with soil depth (Figure 3c,d). In the most depleted organic layers of mature forests, $\delta^{13}C$ and $\delta^{15}N$ vary in the range from −27.9 to −29.9‰ and from −1.7 to 1.6‰, respectively.

The pyrogenic Q horizon of 1AP was characterized by the opposite response of $\delta^{13}C$ (enrichment) and $\delta^{15}N$ (depletion) to fire impact in comparison with intact organic layers. The soil horizons most enriched in heavy isotopes are the Bs and upper B horizons, where $\delta^{13}C$ ranges from −22.8 to −24.2 ‰ and $\delta^{15}N$ from 6 to 12 ‰. Deep mineral soil OM contains slightly more negative $\delta^{13}C$ and $\delta^{15}N$. There is an apparent relationship between C:N with $\delta^{13}C$ (Figure 4a) and $\delta^{15}N$ (Figure 4b) values, i.e., the decrease of the C:N ratio corresponds to an enrichment of SOM in heavy C and N isotopes. Organic layers composed of plant debris are characterized by the highest C:N ratios and lowest $\delta^{13}C$ values close to the initial C3 plant-derived matter and $\delta^{15}N$ of NO_3 deposited in northern latitudes with precipitation (1 to 3‰).

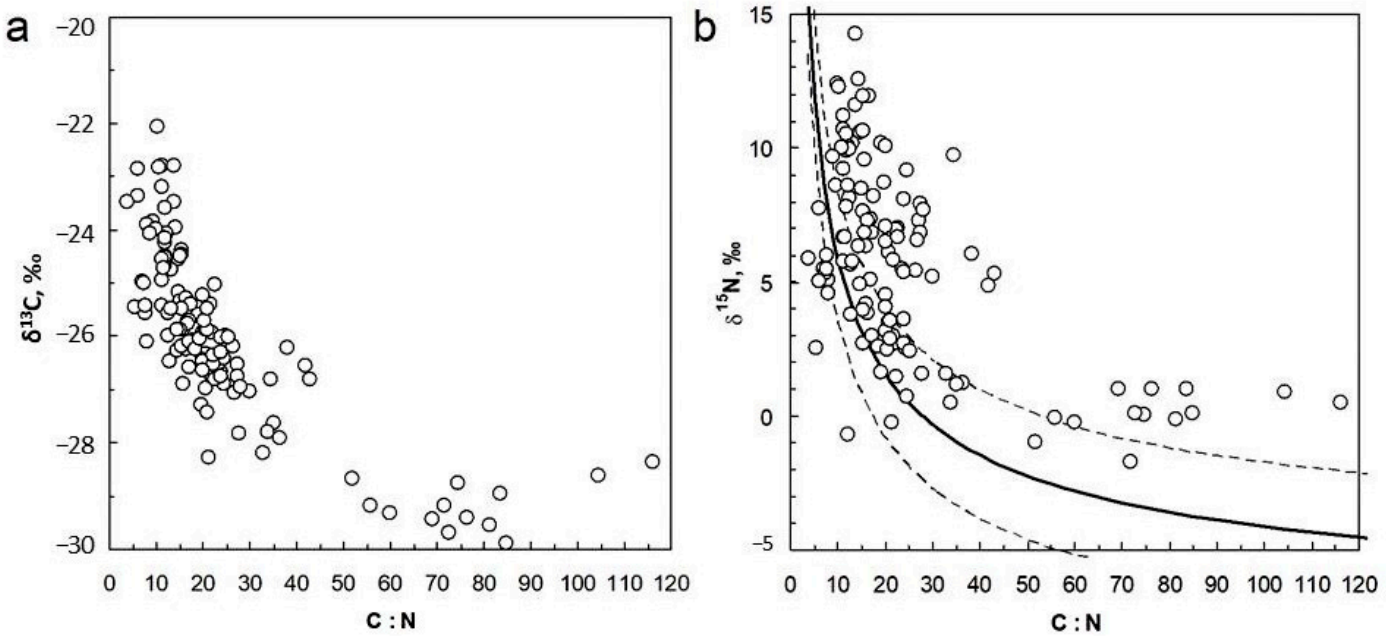

Figure 4. Relationships between C:N ratio and δ^{13}C -SOC (**a**) and δ^{15}N (**b**) in soils (O, E_{pyr}, E, Bs, B horizons) developed under pine forests of Central Siberia affected by wildfires 1–121 years ago. In the figure b, the bold continuous line is a function fitted to the unperturbed soil samples and dashed lines are the range ±2.4‰ as given in Connen et al. 2013 [48].

In mineral soil horizons narrowing C:N ratio with depth, mirroring the mineralization of SOM coincides with the predominant loss of light isotopes of both C and N. In regard to the relationship between C:N and δ^{15}N, the values of the latter are shown to cover a relatively narrow value at any particular C:N ratio (bold and dashed lines on Figure 3b) in soils with little or no perturbation of the N cycle by the creation of new leaks or supplies of N [48]. Soil samples above the uncertainty envelope (set at ±2.4‰) indicate an accelerated N loss, whereas samples below indicate an accelerated N gain. Our findings demonstrated that the largest portion of δ^{15}N values of Central Siberian Podzols lie above the uncertainty envelope (Figure 3d), demonstrating predominantly net losses of N as shown previously for frequently fire-affected soils of Yakutia (Eastern Siberia) [46].

The fire impact and long-term changes of SOM properties (C:N ratio) (Figure 5a), δ^{13}C (Figure 5b) and δ^{15}N (Figure 5c) in the upper 30 cm of soil (E_{pyr}, E and Bs horizons) during a stand restoration (1–121 year after a fire) was most evident in the eluvial horizons (E_{pyr} and E). Spodic Bs horizons of studied soils did not demonstrate significant time-related differences in SOM properties.

The C:N ratios in the E_{pyr} and E horizons of the recently fire-affected plot 1AP was 1.7-fold lower ($p < 0.05$) in comparison to older age plots (23AP and older) (Figure 5a). The SOC in E_{pyr} and E horizons was enriched by heavy isotopes right after a fire (1AP) and δ^{1}3C tended to decrease in both horizons up to 23 years since a fire impact (23AP), then stabilizing at values −26.3 ± 0.3‰ (45AP, 79AP and 121AP) (Figure 5b). SOM δ^{15}N has appeared less affected by fire. Only E_{pyr} horizons showed 1.5–3.0‰ lower δ^{15}N values in the 1AP plot in comparison to older age plots. Recovery to pre-fire values occurred already in plot 23AP (Figure 5c), though the mid-age plot 45AP still demonstrated depletion in heavy isotopes.

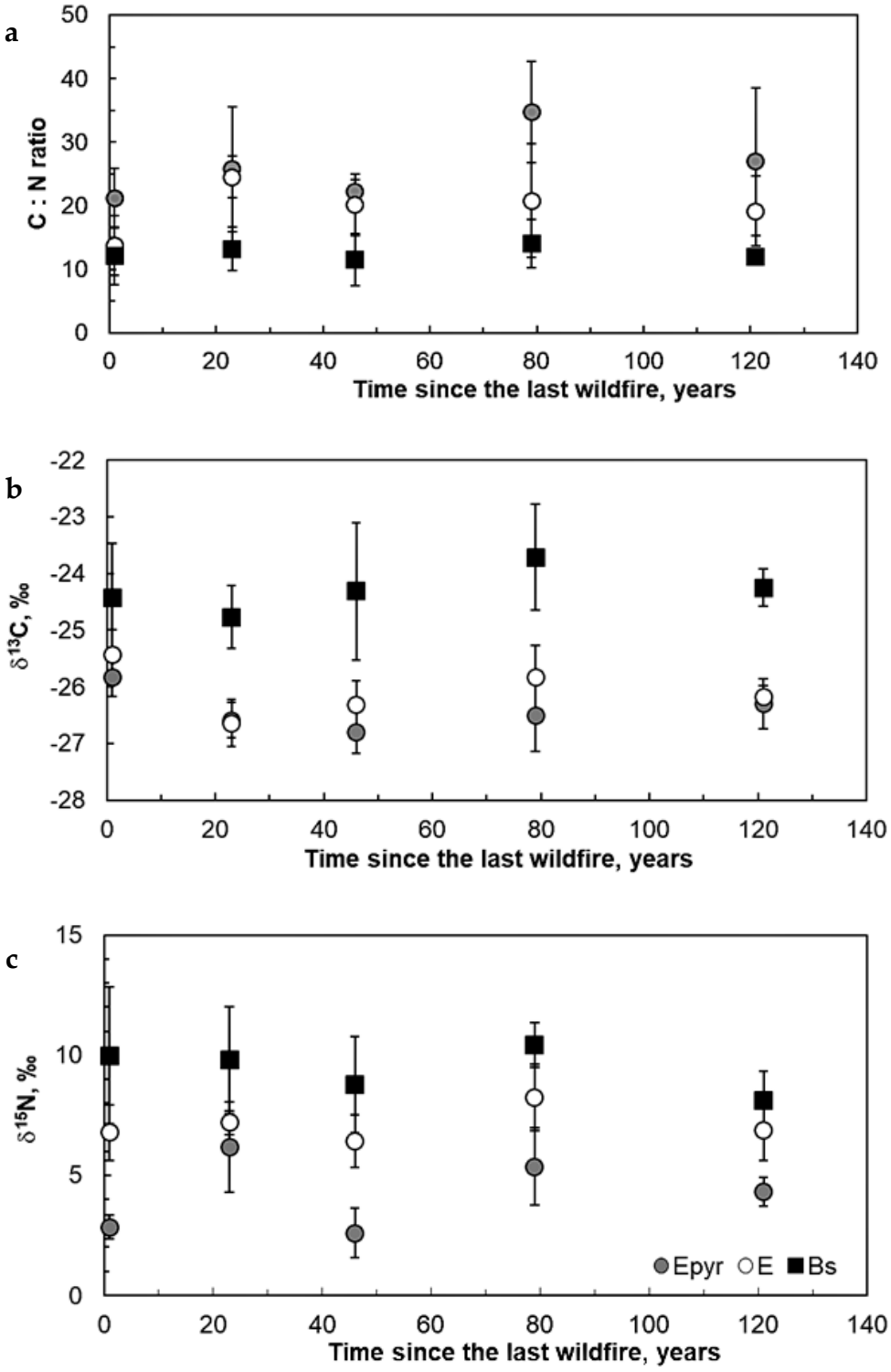

Figure 5. Post-fire dynamics of C:N ratio. (**a**), δ^{13}C-SOC (**b**) and δ^{15}N (**c**) in different soil genetic horizons: E_{pyr}, E (eluvial) and Bs (illuvial).

Organic horizons of the studied soils contain the largest concentrations of WSOC and WSON. Mineral horizons contain sufficiently less WSOC and WSON than organic horizons (Figure 6). It was found that the WSOC content in the area 1AP in the Q_{pyr} horizon was only 0.5 mg g^{-1}, and the WSON content was 0.04 mg g^{-1}. The maximum WSOC content was revealed in the organic horizons of the soil 45AP. The content of WSOC in the organic horizons of plots 23AP and 45AP were 1.5–5.7 mg g^{-1}; the content of WSON varied from

0.07 to 0.26 mg g^{-1}. The content of water-soluble organic carbon in the E horizons of the soils of the studied areas was in the range of 0.08–0.10 mg g^{-1}. For sites 121 years after the last fire, lower contents of WSOC were found in the organic horizon (1.3–2.2 mg g^{-1}). However, in the E_{pyr} of the soil of the plot 121 years after a fire, the maximum increase in the content of WSOC (0.12 mg g^{-1}) was revealed.

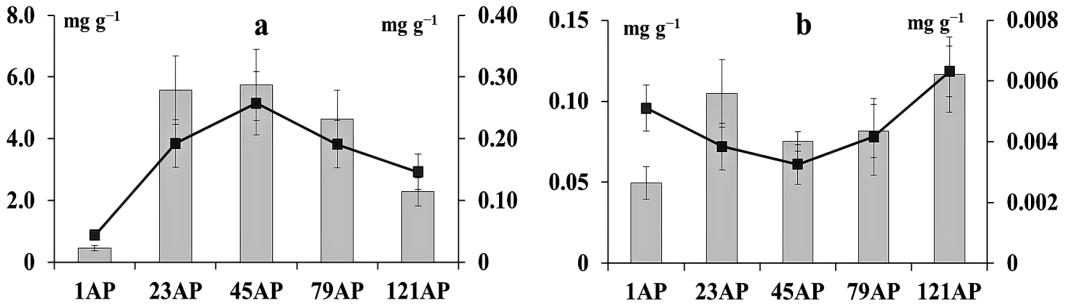

Figure 6. Water soluble organic matter at organic (**a**) and E_{pyr} (**b**) horizons. Columns—water soluble organic carbon (WSOC) on the left scale; line—water soluble organic nitrogen (WSON) on the right scale.

3.5. Content of PAHs of Soils

PAHs were studied in the organic and topsoil mineral horizon (E_{pyr}) (Table 3) because PAHs were absent in the deeper mineral horizons [49].

We found a high content in all of the study horizons. The highest content was found for the 1AP soil. In the horizons of this soil, the PAH content reaches up to 3180 ng g^{-1}. There was a natural decrease in the mass fraction of PAHs with the time from the last fire event (Figure 7). An amount of 2–4 nuclear PAHs were prevalent in the organic horizons. The contribution of light structures to the total mass fraction of PAHs in organic horizons ranged from 80% in older burning sites to 95–96% in areas burned recently. The proportion of 2-nuclear PAHs decreased with age, with an increase in the age of the burning sites from 66 to 20%. The proportion of 5–6 nuclear PAHs increased.

The PAH content correlates with the total nitrogen content (r = 0.99, $p < 0.05$). A high correlation was found between total nitrogen with almost all PAHs (r = 0.51–0.99, $p < 0.05$). In addition, a reliable polynomial trend of decreasing PAHs over time after the last fire in the organic horizons (R^2 = 0.98) and E_{pyr} (R^2 = 0.91) has been established (Figure 7a,b). Significant correlations were found between the time after the fire and the sum mass fraction of PAHs in the organic horizon (r= –0.71, p<0.05) and individual PAHs (r = −0.92 to r = 0.42, $p < 0.05$). For the pyrogenic mineral horizon E_{pyr}, we also found a negative relationship between age after a fire and the ∑PAH content in the is (r = −0.71, $p < 0.05$). With individual PAH compounds, the correlation coefficient varied: r = −0.69, . . . , 0,47, $p < 0.05$.

We calculated the series of PAH diagnostic ratios, which allowed us to determine the origin of the PAHs in soil: ANT/(ANT+PHE), PHE/ANT, (PYR+FLA)/(CHR+PHE), FLA/PYR, (PYR+BaP)/(PHE+CHR) and BaA/228 [50–54]. At the same time, these ratios were found to not be applicable for the studied soils. The ratios (PYR+BaP)/(PHE+CHR), (PYR+FLA)/(CHR+PHE) and BaA/228 showed a petrogenic origin of the PAHs in the burnt soils. The ratios PHE/ANT and ANT/(ANT+PHE) revealed a pyrogenic origin only for Qpyr(1AP) PAHs collected from the soil affected by fire 1 year ago. The ratio FL/PYR also inadequately reflected the origin of PAHs in this soil demonstrated petrogenic origin.

PAH ratios could demonstrate changes depending on the time from the last fire. For example, (PYR+BaP)/(PHE+CHR) was usually lower in the organic Q_{pyr} (Oe, $_{pyr}$) horizons than in the E_{pyr} horizons in old fire areas, while the opposite is typical for young burnt areas. The time patterns were also found for the ratio PHE/ANT, decreasing in the Q_{pyr} horizons compared to E_{pyr} in recent fire areas, and increasing in old fire areas.

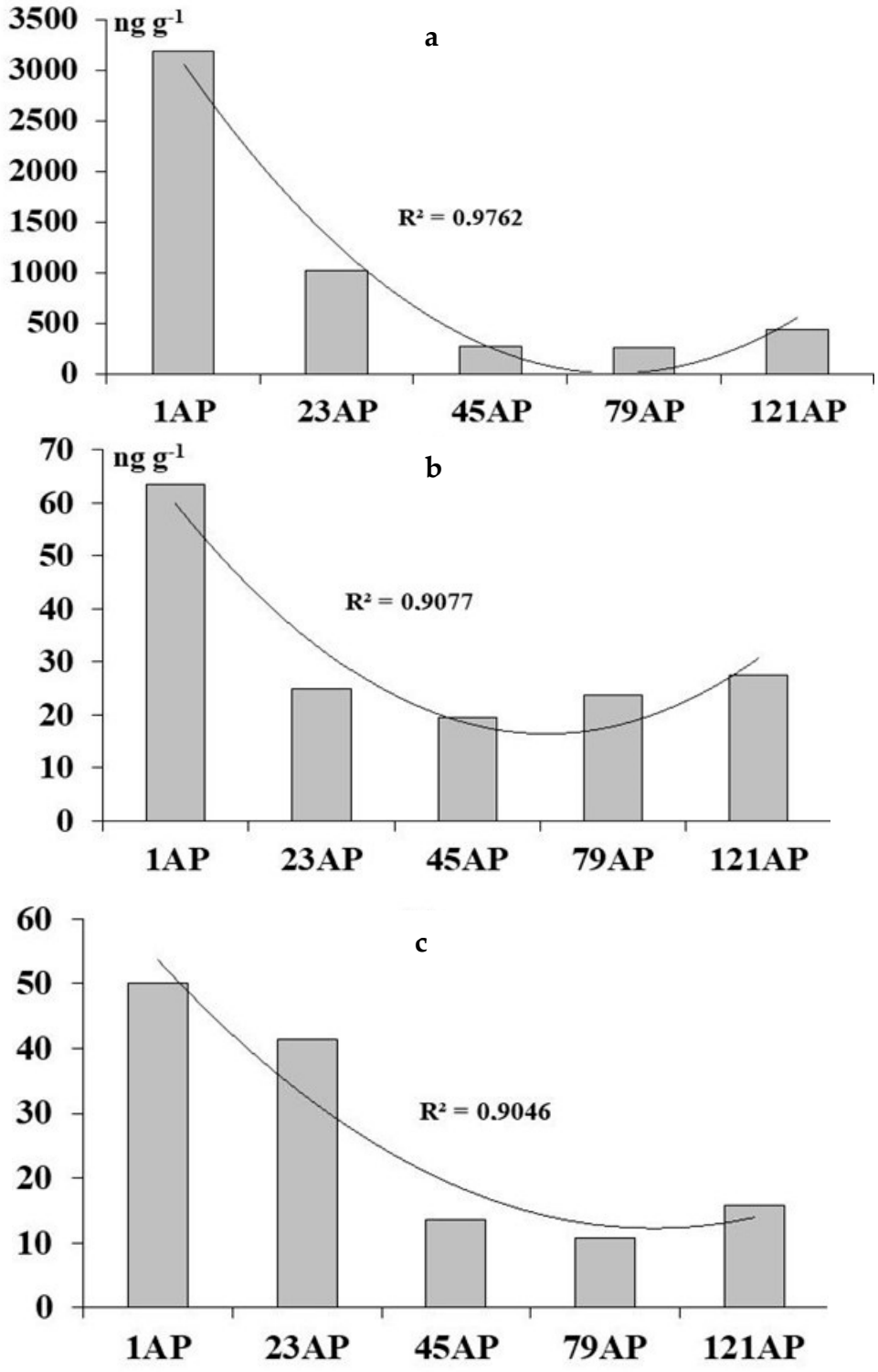

Figure 7. The total content of PAHs in the organic layer (**a**) and E_{pyr} (**b**) of the studied soils. (**c**)—index of pyrogenic activity (IPA). The trend line is polynomial.

We have calculated a new pyrogenic activity index—IPA (Table 4, Figure 7c). The coefficient was the ratio ∑ PAHs at the organic horizon to ∑ PAHs at the upper mineral horizon. The IPA values gradually decrease in the time range after the fire from 50 at the 1 site to 11–16 at the 79 and 121 sites.

Table 4. PAH content at the upper soil horizons, ng g^{-1}.

Site	Horizon	Depth, cm	2-Ring			3-Ring			4-Ring			5-Ring				6-Ring		∑PAHs	IPA *
			NP	ACE	FL	PHE	ANT	FLA	PYR	BaA	CHR	BbF	BkF	BaP	DahA	BghiP	IcdP		
1AP	Q_{pyr}	0–1	2007	–	97.2	424.3	59.9	36.8	58.8	–	305.6	64.4	11.8	48.2	58.8	7.6	–	3180.6	50.0
	E_{pyr}	1–6	14	–	1.0	39.0	0.3	1.9	1.8	–	5.1	–	–	–	–	–	–	63.5	
23AP	Oe_{pyr}	1–3	581	–	20.4	250.4	14.0	25.8	47.2	–	42.7	11.5	5.6	10.8	13.4	1.9	–	1024.6	41.3
	E_{pyr}	3–8	4.3	–	2.0	12.1	0.7	3.1	2.0	0.2	0.3	–	–	–	–	–	–	24.8	
45AP	Oe_{pyr}	3–5	127	–	7.8	75.6	3.9	17.1	5.0	2.0	9.2	7.3	2.0	5.3	3.4	–	–	266.1	13.6
	E_{pyr}	5–11	6.5	–	1.3	6.7	0.4	2.6	0.8	0.3	–	–	–	–	–	–	–	19.6	
79AP	Oe_{pyr}	1–2	75	–	7.0	121.3	5.2	9.5	5.4	1.5	2.5	6.1	3.2	3.6	14.7	1.8	–	256.6	10.8
	E_{pyr}	2–6	8.9	–	1.2	6.8	0.3	3.5	2.1	–	–	–	–	–	–	–	–	23.8	
121AP	Oe_{pyr}	2–4	191	–	9.0	94.5	3.8	8.8	4.0	0.8	22.8	62.0	0.9	5.8	29.3	–	–	432.7	15.7
	E_{pyr}	4–10	13.2	–	0.7	7.5	1.0	1.7	0.7	0.4	2.2	–	–	–	–	–	–	27.5	

Note: 2–4 nuclear PAHs (NP—naphthalene, ACE—acenaphthene, FL—fluorine, PHE—phenanthrene, ANT—anthracene, FLA—fluoranthene, PYR—pyrene, BaA—benzo[a]anthracene, CHR—chrysene), 5–6 nuclear PAHs (BbF—benzo[b]fluoranthene, BkF—benzo[k]fluoranthene, BaP—benzo[a]pyrene, DahA—dibenzo[a,h]anthracene, BghiP—benzo[g,h,i]perylene, IcdP—indeno [1, 2, 3-c, d]pyrene), * IPA–ratio ∑ PAHs at organic horizon to ∑ PAHs at upper mineral horizon (E_{pyr}), dash—below the definition limit.

4. Discussion

4.1. Vegetation Dynamics, Morphological and Chemical Soil Properties

The species diversity and total projective cover of ground vegetation layers of plant communities depend on the age of the last fire. The cover of the herb-dwarf shrub layer was minimal immediately after the fire and further increased during post-pyrogenic succession. The restoration of the moss-lichen layer after-fire occurs in much faster rates than vascular plants. Recently, it was found that the middle-term post-fire recovery rate of the boreal moss-lichen layer is faster than the other layers of plant communities both in terms of species diversity [55] and biomass [56]. In this study, we also revealed faster moss-lichen layer restoration already at the 23-year site with it maintaining a stable state during further succession.

The investigated soils are characterized by a typical morphological profile (O–E–Bs–B) with the pyrogenic features in the upper genetic horizons (O_{pyr}, E_{pyr}), which is similar to the literature data on Podzols of different regions of the Russian Federation [9,57,58]. Under low intensity surface fires, changes in the vegetation and the burning of the organic horizon result in the formation of the pyrogenic Q_{pyr} horizon. Similar pyrogenic soil properties have been noted in the soils of the Baikal region [59], which indicated the influence of surface fires on the transformation of organic soil horizons into new specific pyrogenic horizons.

The capacity and water content of organic soil horizons are significant indicators of forest soil restoration after fire impact. The moss-lichen layer of plants has not yet formed in the soils of young burnt areas. In these areas, the minimum values of humidity and thickness of organic horizons were revealed. The increasing of the thickness of organic horizons and the moisture content of organic soil horizons is found with the time that has passed since the last fire. The exception is the site 79AP, in which the moisture is lowest from the studying sites. In general, post-pyrogenic successions of lichen pine forests are characterized by a gradual increase in the proportion of mosses (primarily *Pleurozium schreberi*). The average thickness of forest litter at the stage of stabilization after fires for pine forests is 7.5–8.5 cm, which corresponds to the results published previously [60].

The degree of transformation of soil organic compounds is determined by the combustion temperature [24]. According to [25,61], natural biopolymers change already at temperatures of about 300 °C, and the formation of ash and coal begins. Coal particles play a significant role in the genetic horizons of soils for diagnosing past-fires [19,62]. Pyrogenic morphological features (charcoal, soot, partially charred residues) can be preserved both in organic, and in the upper mineral, soil horizons. The presence of pyrogenic signs is usually denoted by adding a «$_{pyr}$» to the designation of the name. In all the studied podzols, the presence of coal particles in the litter and eluvial horizons was revealed, which persisted for a long time after the fire, even after 121 years.

The Podzols of the studied areas are characterized by high acidity, typical for boreal landscape soils. A decrease in the acidity (increase at pH values) of organic horizons occurred in the first year after the fire, corroborating earlier observations in temperate and boreal forests [63,64]. Higher pH values are due to saturation by ash elements [21] and a reduction in the content of water soluble organic acids. In addition, coal particles are formed in which low-molecular-weight organic compounds can be absorbed [65,66]. In the course of succession, the vegetation of the ground cover is restored, and soil acidification is observed.

The most conservative properties of the studied soils, such as texture, are slightly subject to changes during low-intensity fires. Fire impacts on the SSA of organic horizons is most clearly seen in the first years after the fire [35]. The influx of coal particles with a high surface in the first years after a fire can have a significant impact on the chemical composition of soil water. With further succession and the supply of fresh plant material, the values decrease significantly.

4.2. Soil Organic Matter of Studied Soils

Bulk soil organic C and total N concentrations are among parameters that are regularly assessed in forest ecosystem research to analyze soil organic matter (SOM) pools and ecosystem development. Furthermore, stoichiometric ratios such as the carbon:nitrogen (C:N) ratio and stable isotope composition ($\delta^{13}C$ and $\delta^{15}N$) of SOM also provide a powerful tool for investigating spatial and temporal SOM dynamics and particularly, SOM turnover and stability, including fire disturbances [67–70].

Forest soils are characterized by the continuous inputs of fresh plant litter and roots that are steadily mixed and undergo microbial decomposition downward the soil profile [71–73]. Our data clearly demonstrate that Albic Podzols under pristine and fire-affected pine forests are supplied by a litter fall containing wide C:N and ^{13}C and ^{15}N depleted organic matter, as it was shown earlier for boreal and temperate forests [68,70]. With increasing soil depths and the aging of SOM [74], the content of C and N and C:N ratios in forest soils tend to decrease, and, in opposite, $\delta\ ^{13}C$ and $\delta\ ^{15}N$ show a trend toward enrichment by heavier isotopes [67–70]. These depth patterns are specific in Albic Podzols as the eluvial E horizon lying below an organic layer is strongly depleted by C and N in comparison to the deeper illuvial Bs horizon [15]. Despite this fact, $\delta^{13}C$ and $\delta^{15}N$ values in studied Podzols under pine forests demonstrate steady enrichment with soil depth, with relatively stable values in deep B and C horizons. It suggests the most intense microbial processing of plant residues in the upper 50 cm of soil (i.e., E and Bs horizons), resulting in the preferential release of 13C-depleted molecules [70,72]. The increase of ^{15}N in the soil depth gradient is the result of isotopic fractionation during SOM mineralization and the removal of depleted inorganic N via plants, microbes or leaching related to microbial driven processes and particularly, nitrification responsible for losses of ^{15}N-depleted nitrate [75–79]. The greater contribution of microbial derived $\delta^{13}C$- and $\delta^{15}N$ -enriched matter in deep soil [67,72,80] is another factor responsible for heavier isotopic content of subsoil SOM. On the other hand, stabilization or even decrease of $\delta^{13}C$ and $\delta^{15}N$ in deep SOM of Albic Podzols might reflect specifics of deep SOM turnover in this environment and requires further research. Thus, both $\delta^{13}C$ and $\delta^{15}N$ values are found mechanistically linked through the SOM mineralization and microbial processing, highlighting the importance of both parameters to determine the degree of organic matter turnover in soil [68,69,81–84].

Forest fires affect the total amount and cycling of C and N in an ecosystem, which are stored in the forest floor [85–87]. Common shifts in isotopic composition of remaining SOM, i.e., enrichment of topsoil with heavier isotopes [80], are demonstrated due to the predominant burning of the depleted top litter layer [86,88,89]. In regard to ^{15}N discrimination against heavier isotopes during volatilization of N [78] or the enhanced nitrification process and nitrate, leaching occurred after a fire impact and was shown in several boreal and temperate forests [48,70]. The wildfires in studied pine forests had relatively minor effects on the SOC content and isotopic composition of C and N in the remaining organic

layer after a fire, which is likely modulated by vegetation composition, fire intensity and severity [90]. On the other hand, the remaining OM on the mineral soil of studied pine forests demonstrated a narrower C:N ratio, which is usually significantly reduced after a wildfire, as a result of the combustion of upper fresher plant material's Oi layer [70,85,88].

Despite the changes in subsoil C and N content rarely being observed after a fire [70], the major consequence of periodic fires in pine forests is the formation of a specific E_{pyr} horizon relatively enriched by C and having a wider C:N ratio, in comparison to typical E horizons of Podzols. These findings reflect the accumulation of charcoal, which in part might represent the ecosystem legacy carbon [91] and likely the most resistant pool of C in studied ecosystems which can contribute to C sequestration over longer (i.e., decadal to millennial) time scales [92]. The post-fire dynamics of the C:N ratio and isotopic composition of SOM in E and E_{pyr} horizons demonstrated similar patterns of increasing C:N ratios and depletion of ^{13}C with time, reflecting an input of fresh OM. Changes in SOM were much less apparent in deeper soil, and the Bs horizon did not demonstrate any changes after the fire and further with post-fire succession.

Simultaneous measurements of $\delta\ ^{15}N$, N and the C:N ratio in SOM are demonstrated to provide the indication for a perturbation to N cycling caused by a fire or anthropogenic influences [48,78,79]. Particularly, changes in N cycling are mostly related with the loss or gain of ^{15}N-depleted substances which then result in larger or smaller $\delta^{15}N$ values of SOM at the observed C:N ratio [48]. An accelerated mineralization of soil organic matter may increase or decrease $\delta^{15}N$ in relation to respective C:N ratios, which in turn reflects recent or past soil perturbations. Generally, soil $\delta^{15}N$ appearing above the uncertainty value (set at $\pm 2.4‰$) supposes an accelerated N loss, and soil $\delta^{15}N$ below indicates an enhanced N gain. Analyzed Albic Podzol soils (Figure 4b) showed common patterns of past fire perturbations of SOM turnover; the majority of samples appeared above this uncertainty envelope, demonstrating the predominant net loss of N in studied pine forests.

It was found that the content of WSOC and WSON in post-pyrogenic organic horizons (Q_{pyr}) of «young» fire sites significantly decreases. The patterns of carbon content in water-soluble compounds after fires are determined by two main factors. The concentration of water-soluble carbon compounds is largely related to the excretions of ground cover plants. In the course of post-pyrogenic successions, this factor will be decisive. Fires lead to the death of ground cover plants, which in turn contributes to a significant decrease in the concentration of water-soluble carbon compounds [93]. As the plants of the top cover are restored, there is a gradual increase in the content of carbon and nitrogen of water-soluble organic compounds due to the input of organic substances [22]. The second factor is related with the coals formed during the fire. Coals have a significant surface area and can absorb a significant part of organic compounds entering the soil [94–96].

Densiometric fractionation of soil organic matter is devoted to the consistent simplification of the catfish system and the production of functional pools of organic matter with characteristic properties. Less destructive methods are used to isolate SOM fractions with specific properties [46,47,97,98]. The method makes it possible to divide the soil into fractions differing in composition, activity of participation in the biological carbon cycle and residence time in the soil into active "young" carbon, which is part of the light fractions of free ($fPOM_{< 1.6}$) and occluded ($oPOM_{< 1.6}$) organic matter, and slow "old" carbon of the heavy fraction ($MaOM_{> 1.6}$) [99–101]. In the composition of the densimetric fractions of the studied upper mineral soil horizons, heavy fractions ($MaOM_{> 1.6}$) predominate, which corresponds to the literature data [102–104]. The isolated densitometric fractions have some differences in the content of total organic carbon. Fractions $fPOM_{< 1.6}$ and $oPOM_{< 1.6}$ are characterized by higher carbon concentrations. The increase in carbon in the light fractions may be due to the enrichment of these horizons with pyrogenically modified parts of the litter. Pyrogenic carbon (PyC) is considered to be one of the most stable carbon deposition pools from the atmosphere [105]. We have suggested that light fractions can concentrate pyrogenic carbon better than heavy fractions. Some authors note in their works that pyrogenesis products are mainly part of light fractions [7,106].

It is known that fires change the chemical composition of organic matter, and lead to the enrichment of soils with pyrogenic black carbon (PyC) [107–109]. Our results on WSOC are close to the data of Ide with co-authors [58], and it can be assumed that some of the compounds formed during fires may have good solubility in water and affect the composition of WSOC in soils [110,111]. However, this requires additional studies of dynamic contents of the molecular composition of WSOC after fire impact.

4.3. Content of PAHs of Soils

Forest fires lead to the formation of large amounts of PAHs during combustion [36,112,113]. We found similar patterns in PAH formation of organic horizons of Central Siberia and postpyrogenic boreal soils of the European North of Russia [12]. It should be noted that PAHs are quite good indicators of pyrogenic effects. The high content of PAHs in the organic horizon of the 1AP plot (one year after fire) supports the fact that these compounds have not yet been actively included in the biological cycle and are not decomposed in the process of photochemical destruction. This fact confirms that in the soils of the 1AP, PAHs are represented by two-nuclear structures by 66%, mainly naphthalene, which are most easily degraded. Other researchers [36,112,113] showed a high contribution of light PAHs to the ∑ PAHs in the organic horizons immediately after fire with a following strong decline during the year. Our results indicate that levels of light PAHs in the litter remain high 10–16 years after a fire [12]. The decomposition of naphthalene, the most vaporized and exposed to microbiological decomposition, results in the decline of the light PAHs fraction in soils with older fires. Microbiological decomposition of PAHs follows the pattern of successive rings' destruction. Light structures decompose first [67,114–116]. In the case of the site 121AP, an active decomposition of 3–4 nuclear PAHs to naphthalene has led to the increase of its concentration in the organic soil horizon. Heavy PAHs degraded to a lesser extent, and their proportion in the ∑PAHs was quite high (23%).

Factors affecting the pyrogenic formation of light and heavy PAHs are different [36,113]. The formation of 2–4 nuclear PAHs depends on combustion conditions, such as oxygen access, high temperature and exposure time. The formation of 5–6 nuclear structures mainly depends on the plant composition and type of burnt organic horizon. For instance, the organic horizon formed during *Pinus nigra* combustion contained less PAHs than those from *Pinus pinaster* [34]. The decrease in the mass fraction of PAHs in organic horizons was due to the effect of decomposition and restoration of vegetation, which leads to a change in the pyrogenic-modified Q_{pyr} horizon. At the same time, the PAH content per unit mass at the organic horizons becomes less. Coefficients recommended for identifying the contribution of pyrogenic and pedogenic PAHs [50–54] were not correlated with the time of the last fire. This result may be due to the fact that these ratios of PAHs were calculated for the snow cover [50,117], and may not be completely suitable for soils. The increasing PAHs contents in soils could also be based on the processes of the anthropogenic burn of oil and gas. Thus, the natural biomass combustion PAHs could be included in the «petrogenic» PAHs.

The relationships between PAH ratios and fire age made it possible to calculate a new index—index of pyrogenic activity (IPA), most accurately reflecting the effect of the fire age on the composition of polyarenes in soils subjected to pyrogenic action. For forests affected by fires 1 and 23 years ago, the highest IPA ratio was revealed.

PAHs, especially heavy structures, are poorly water soluble [118,119]. Low migration of PAHs throughout the soil profile results in low PAH content in the mineral soil horizons under study. Minimal amounts of heavy PAHs were present in the mineral horizons. This result is in line with other studies [120], including those for podzols in the first months after the fire [49]. At the same time, there are few studies that demonstrate PAHs' migration into the underlying soil horizons [121].

5. Conclusions

Our study clearly shows that pyrogenic changes in the upper genetic horizons of Albic Podzols were saved over a long period of time from 1 year to 121 years after a fire. As a result of the study, it is shown that pine forests of the Eastern edge of western Siberia are exposed to fires, which affect the morphological and chemical properties of soils, and increase the contribution of pyrogenically modified components to the composition of the soil organic matter. The main morphological changes in soils after the fire are the formation specific soil horizons Q_{pyr} and preservation pyrogenic sings at the Oe, $_{pyr}$ and E_{pyr} horizons, which are saturated with pyrogenesis products (coals, soot). Pyrogenic inclusions are well preserved and diagnosed 121 years after the passage of the fire. The influence of forest fires in the early years on the chemical properties of Albic Podzols is manifested in a decrease in acidity, a decrease in the content of water-soluble forms of carbon and nitrogen and an increase in the content of light PAHs in organic and mineral horizons; there is also enrichment in heavier isotopes ($\delta^{13}C$). A new indicator is proposed—the pyrogenic activity index (IPA), which most accurately reflects the influence of the age of the last fire on the composition of polyarenes in soils exposed to pyrogenic effects.

Supplementary Materials: The following supporting information can be downloaded at: https://www.mdpi.com/article/10.3390/fire6020067/s1, Figure S1: Photos of landscapes and soil profiles of studied plots.

Author Contributions: Conceptualization, A.A.D. and A.S.P.; methodology, A.A.D.; software, A.V.P.; validation, V.V.S.; formal analysis, E.V.Y., D.A.S., E.Y.M., A.A.D. and V.V.S.; investigation, A.A.D., A.S.P. and V.V.S.; resources, A.A.D. and A.S.P.; data curation, A.A.D. and A.S.P.; writing—original draft preparation, A.A.D., V.V.S., Y.A.A.D. and A.S.P.; writing—review and editing, A.A.D. and A.S.P.; visualization, A.A.D. and A.S.P.; supervision, A.A.D.; project administration, A.A.D.; funding acquisition, A.A.D. All authors have read and agreed to the published version of the manuscript.

Funding: This work was supported by the Russian Foundation for Basic Research (RFBR) under Grant No. 19-29-05111 mk.

Institutional Review Board Statement: Not applicable.

Informed Consent Statement: Not applicable.

Data Availability Statement: The data presented in this study are available upon request from the corresponding author.

Conflicts of Interest: The authors declare no conflict of interest.

References

1. Sannikov, S.N. *Ecology and Geography of Scots Pine Natural Regeneration*; Nauka: Moscow, Russia, 1992; p. 264. (In Russian)
2. Dymov, A.A.; Startsev, V.V.; Gorbach, N.M.; Pausova, I.N.; Gabov, D.N.; Donnerhack, O. Comparison of the Methods for Determining Pyrogenically Modified Carbon Compounds. *Eurasian Soil Sci.* **2021**, *54*, 1668–1680. [CrossRef]
3. Gorbach, N.; Kutyavin, I.; Startsev, V.; Dymov, A. Dynamics of fires in the northeast of the European part of Russia in the Holocene. *Theor. Appl. Ecol.* **2021**, *3*, 104–110. (In Russian) [CrossRef]
4. Bond-Lamberty, B.; Peckham, S.D.; Ahl, D.E.; Gower, S.T. Fire as the dominant driver of central Canadian boreal forest carbon balance. *Nature* **2007**, *450*, 89–92. [CrossRef] [PubMed]
5. Vedrova, E.F.; Evdokimenko, M.D.; Bezkorovainaya, I.N.; Mukhortova, L.V.; Cherednikova, Y.S. Carbon reserves in organic matter of postfire pine forests in southwestern lake Baikal basin. *Lesovedenie* **2012**, *1*, 3–13. (In Russian)
6. Santin, C.; Doerr, S.H. Fire effects on soils: The human dimension. *Philos. Trans. R. Soc. B Biol. Sci.* **2016**, *371*, 20150171. [CrossRef]
7. Maksimova, E.; Abakumov, E. Soil organic matter quality and composition in a postfire Scotch pine forest in Tolyatti, Samara region. *Biol. Commun.* **2017**, *62*, 169–180. [CrossRef]
8. Gabbasova, I.M.; Garipov, T.T.; Komissarov, M.A.; Suleimanov, R.R.; Sidorova, L.V.; Suleimanov, A.R.; Nazyrova, F.I.; Suyundukov, Y.T.; Khasanova, R.F.; Komissarov, A.V. The impact of fire on properties on steppe soils in trans-ural region. *Eurasian Soil Sci.* **2019**, *52*, 1598–1607. [CrossRef]
9. Nadporozhskaya, M.A.; Pavlov, B.A.; Mirin, D.M.; Yakkonen, K.L.; Sedova, A.M. The influence of forest fires on the formation of the profile of podzols. *Biosfera* **2020**, *12*, 32–44. (In Russian) [CrossRef]

10. Dymov, A.A.; Grodnitskaya, I.D.; Yakovleva, E.V.; Dybrovskiy, Y.A.; Kutyavin, I.N.; Startsev, V.V.; Milanovsky, E.Y.; Prokushkin, A.S. Albic Podzols of boreal Pine forests of Russia: Soil organic matter, physico-chemical and microbiological properties across pyrogenic history. *Forests* **2022**, *13*, 1831. [CrossRef]
11. Bezkorovainaya, I.N.; Ivanova, G.A.; Tarasov, P.A.; Sorokin, N.D.; Bogorodskaya, A.V.; Ivanov, V.A.; Konard, S.G.; McRae, D.J. Pyrogenic Transformation of Pine Stand Soil in Middle Taiga of Krasnoyarsk Region. *Contemp. Probl. Ecol.* **2005**, *12*, 143–152.
12. Dymov, A.A.; Gabov, D.N.; Milanovskii, E.Y. ^{13}C-NMR, PAHs, WSOC and repellence of fire affected soils (Albic Podzols) in lichen pine forests, Russia. *Environ. Earth Sci.* **2017**, *76*, 275. [CrossRef]
13. Dymov, A.A. *Soil Successions in Boreal Forests of the Komi Republic*; GEOS: Moscow, Russia, 2020; p. 336, (In Russian). [CrossRef]
14. Nachtergaele, F. Soil taxonomy—A basic system of soil classification for making and interpreting soil surveys: Second edition, by Soil Survey Staff, 1999, USDA–NRCS, Agriculture Handbook number 436, Hardbound. *Geoderma* **2001**, *99*, 336–337. [CrossRef]
15. Van Ranst, E. *Soil Atlas of Europe*; European Commission: Brussels, Belgium, 2005; p. 128.
16. Lundstrom, U.S.; van Breemen, N.; Bain, D. The podzolization process. *A review. Geoderma* **2000**, *94*, 91–107. [CrossRef]
17. IUSS Working Group WRB. *World Reference Base for Soil Resources 2014, Update 2015. International Soil Classification System for Naming Soils and Creating Legends for Soil Maps. World Soil Resources Reports No. 106*; FAO: Rome, Italy, 2015.
18. Ivanov, A.L.; Shoba, S.A. (Eds.) *Unified State Register of Soil Resources of Russia. Version 1.0*; Dokuchaev Soil Science Institute: Moscow, Russia, 2014; p. 768. (In Russian)
19. Krasnoshchekov, Y.N. Postpyrogenic variability of litter in mountain forest of Baikal region. *Eurasian Soil Sci.* **2019**, *52*, 258–270. [CrossRef]
20. Loiko, S.V.; Kuzmina, D.M.; Dudko, A.A.; Konstantinov, A.O.; Vasilyeva, Y.U.A.; Kurasova, A.O.; Lim, A.G.; Kulizhsky, S.P. Charcoals of albic podzols of the middle taiga of Western Siberia as indicator of ecosystem history. *Eurasian Soil Sci.* **2022**, *55*, 176–192. [CrossRef]
21. Pereira, P.; Úbeda, X.; Martin, D. Fire severity effects on ash chemical composition and water-extractable elements. *Geoderma* **2012**, *191*, 105–114. [CrossRef]
22. Pellegrini, A.F.A.; Harden, J.; Georgiou, K.; Hemes, K.S.; Malhotra, A.; Nolan, C.J.; Jackson, R.B. Fire effects on the persistence of soil organic matter and long-term carbon storage. *Nat. Geosci.* **2021**, *15*, 5–13. [CrossRef]
23. Chebykina, E.; Abakumov, E. Essential Role of Forest Fires in Humic Acids Structure and Composition Alteration. *Agronomy* **2022**, *12*, 2910. [CrossRef]
24. Bird, M.I.; Wynn, J.G.; Saiz, G.; Wurster, C.M.; McBeath, A. The Pyrogenic Carbon Cycle. *Annu. Rev. Earth Planet. Sci.* **2015**, *43*, 273–298. [CrossRef]
25. Bryanin, S.; Kondratova, A.; Abramova, E. Litter Decomposition and Nutrient Dynamics in Fire-Affected Larch Forests in the Russian Far East. *Forests* **2020**, *11*, 882. [CrossRef]
26. Bryanin, S.V.; Danilov, A.V.; Susloparova, E.S.; Ivanov, A.V. Pyrogenic Carbon Pools of the Upper Amur Region. *Contemp. Probl. Ecol.* **2022**, *15*, 777–786. [CrossRef]
27. Santín, C.; Doerr, S.H.; Merino, A.; Bryant, R.; Loader, N.J. Forest floor chemical transformations in a boreal forest fire and their correlations with temperature and heating duration. *Geoderma* **2016**, *264*, 71–80. [CrossRef]
28. Jiménez-Morillo, N.T.; de la Rosa, J.M.; Waggoner, D.; Almendros, G.; González-Vila, F.J.; González-Pérez, J.A. Fire effects in the molecular structure of soil organic matter fractions under Quercus suber cover. *Catena* **2016**, *145*, 266–273. [CrossRef]
29. Kosyakov, D.S.; Ul'Yanovskii, N.V.; Latkin, T.B.; Pokryshkin, S.A.; Berzhonskis, V.R.; Polyakova, O.V.; Lebedev, A.T. Peat burning—An important source of pyridines in the earth atmosphere. *Environ. Pollut.* **2020**, *266*, 115109. [CrossRef] [PubMed]
30. Bird, M.I.; Ascough, P.L. Isotopes in pyrogenic carbon: A review. *Org. Geochem.* **2012**, *42*, 1529–1539. [CrossRef]
31. Glaser, B.; Haumaier, L.; Guggenberger, G.; Zech, W. Black carbon in soils: The use of benzenecarboxylic acids as specific markers. *Org. Geochem.* **1998**, *29*, 811–819. [CrossRef]
32. Brodowski, S.; Rodionov, A.; Haumaier, L.; Glaser, B.; Amelung, W. Revised black carbon assessment using benzene polycarboxylic acids. *Org. Geochem.* **2005**, *36*, 1299–1310. [CrossRef]
33. Guggenberger, G.; Rodionov, A.; Shibistova, O.; Grabe, M.; Kasansky, O.A.; Fuchs, H.; Mikheyeva, N.; Zrazhevskaya, G.; Flessa, H. Storage and mobility of black carbon in permafrost soils of the forest tundra ecotone in Northern Siberia. *Glob. Chang. Biol.* **2008**, *14*, 1367–1381. [CrossRef]
34. Dymov, A.; Gabov, D. Pyrogenic alterations of Podzols at the North-east European part of Russia: Morphology, carbon pools, PAH content. *Geoderma* **2015**, *241*, 230–237. [CrossRef]
35. Dymov, A.; Startsev, V.; Milanovsky, E.; Valdes-Korovkin, I.; Farkhodov, Y.; Yudina, A.; Donnerhack, O.; Guggenberger, G. Soils and soil organic matter transformations during the two years after a low-intensity surface fire (Subpolar Ural, Russia). *Geoderma* **2021**, *404*, 115278. [CrossRef]
36. Rey-Salgueiro, L.; Martínez-Carballo, E.; Merino, A.; Vega, J.A.; Fonturbel, M.T.; Simal-Gandara, J. Polycyclic Aromatic Hydrocarbons in Soil Organic Horizons Depending on the Soil Burn Severity and Type of Ecosystem. *Land Degrad. Dev.* **2017**, *29*, 2112–2123. [CrossRef]
37. Gennadiev, A.N.; Tsibart, A.S. Pyrogenic polycyclic aromatic hydrocarbons in soils of reserved and anthropogenically modified areas: Factors and features of accumulation. *Eurasian Soil Sci.* **2013**, *46*, 28–36. [CrossRef]

38. Ravindra, K.; Bencs, L.; Wauters, E.; de Hoog, J.; Deutsch, F.; Roekens, E.; Bleux, N.; Berghmans, P.; Van Grieken, R. Seasonal and site-specific variation in vapour and aerosol phase PAHs over Flanders (Belgium) and their relation with anthropogenic activities. *Atmos. Environ.* **2006**, *40*, 771–785. [CrossRef]
39. Czimczik, C.I.; Schmidt, M.W.I.; Schulze, E.-D. Effects of increasing fire frequency on black carbon and organic matter in Podzols of Siberian Scots pine forests. *Eur. J. Soil Sci.* **2004**, *56*, 417–428. [CrossRef]
40. Ipatov, V.S.; Mirin, D.M. *Description of Phythocoenosis. Metodical Recommendations*; St. Petersburg State University press: St. Petersburg, Russia, 2008. (In Russian)
41. Oyama, M.; Takehara, H. *Revised Standard Soil Color Charts*, 2nd ed.; Ministry of Agriculture and Forestry: Tokyo, Japan, 1970.
42. Madany, M.H.; Swetnam, T.W.; West, N.E. Comparison of two approaches for determining fire dates from tree scars. *For. Sci.* **1982**, *28*, 856–861.
43. Fritts, H.C. Dendroclimatology and dendroecology. *Quat. Res.* **1971**, *4*, 419–449. [CrossRef]
44. Grissino-Mayer, H.A. Manual and tutorial for the proper use of an increment borer. *Tree-Ring Res.* **2003**, *59*, 63–79.
45. Van Reeuwijk, L.P. (Ed.) *Procedures for Soil Analysis*; Technical Paper 9; ISRIC: Wageningen, The Netherlands, 2002.
46. Grünewald, G.; Kaiser, K.; Jahn, R.; Guggenberger, G. Organic matter stabilization in young calcareous soils as revealed by density fractionation and analysis of lignin—Derived constituents. *Org. Geochem.* **2006**, *37*, 1573–1589. [CrossRef]
47. Cerli, C.; Celi, L.; Kalbitz, K.; Guggenberger, G.; Kaiser, K. Separation of light and heavy organic matter fractions in soil—Testing for proper density cut-off and dispersion level. *Geoderma* **2012**, *170*, 403–416. [CrossRef]
48. Conen, F.; Yakutin, M.V.; Carle, N.; Alewell, C. δ15N natural abundance may directly disclose perturbed soil when related to C:N ratio. *Rapid Commun. Mass Spectrom.* **2013**, *27*, 1101–1104. [CrossRef]
49. Dymov, A.A.; Dubrovsky, Y.A.; Gabov, D.N. Pyrogenic changes in iron-illuvial podzols in the middle taiga of the Komi Republic. *Eurasian Soil Sci.* **2014**, *47*, 47–56. [CrossRef]
50. Yunker, M.B.; Macdonald, R.W.; Vingarzan, R.; Mitchell, R.H.; Goyette, D.; Sylvestre, S. PAHs in the Fraser River basin: A critical appraisal of PAH ratios as indicators of PAH source and composition. *Org. Geochem.* **2002**, *33*, 489–515. [CrossRef]
51. Pies, C.; Yang, Y.; Hofmann, T. Distribution of polycyclic aromatic hydrocarbons (PAHs) in floodplain soils of the Mosel and Saar River. *J. Soils Sediments* **2007**, *7*, 216–222. [CrossRef]
52. Froehner, S.; de Souza, D.B.; Machado, K.; Falcão, F.; Fernandes, C.S.; Bleninger, T.; Neto, D.M. Impact of coal tar pavement on polycyclic hydrocarbon distribution in lacustrine sediments from non-traditional sources. *Int. J. Environ. Sci. Technol.* **2012**, *9*, 327–332. [CrossRef]
53. Tobiszewski, M.; Namieśnik, J. PAH diagnostic ratios for the identification of pollution emission sources. *Environ. Pollut.* **2012**, *162*, 110–119. [CrossRef] [PubMed]
54. Mizwar, A.; Trihadiningrum, Y. PAH Contamination in Soils Adjacent to a Coal-Transporting Facility in Tapin District, South Kalimantan, Indonesia. *Arch. Environ. Contam. Toxicol.* **2015**, *69*, 62–68. [CrossRef]
55. Degteva, S.V.; Dubrovskiy, Y.A. *Forests in the Basin of the Ilych River in the Pechoro-Ilychsky Reserve*; Nauka: St. Petersburg, Russia, 2014; p. 291. (In Russian)
56. Kukavskaya, E.A.; Buryak, L.; Kalenskaya, O.P.; Zarubin, D.S. Transformation of the ground cover after surface fires and estimation of pyrogenic carbon emissions in the dark-coniferous forests of Central Siberia. *Contemp. Probl. Ecol.* **2017**, *10*, 62–70. [CrossRef]
57. Gyninova, A.B.; Dyrzhinov, Z.D.; Kulikov, A.I.; Gyninova, B.D.; Gonchikov, B.N. Post-pyrogenic Evolution of Sandy Soils under Pine Forests in the Baikal Region. *Eurasian Soil Sci.* **2019**, *52*, 414–425. [CrossRef]
58. Ide, J.; Ohashi, M.; Köster, K.; Berninger, F.; Miura, I.; Makita, N.; Yamase, K.; Palviainen, M.; Pumpanen, J. Molecular composition of soil dissolved organic matter in recently-burned and long-unburned boreal forests. *Int. J. Wildland Fire* **2020**, *29*, 541. [CrossRef]
59. Krasnoshchekov, Y.N.; Cherednikova, Y.S. *Postpyrogenic Variability of Forest Soils in the Mountainous Baikal Region*; SBRAS Novosibirsk: Novosibirsk, Russia, 2022; (In Russian). [CrossRef]
60. Gorshkov, V.V.; Stavrova, N.I.; Bakkal, I.Y. Post-fire restoration of forest litter in boreal pine forest. *Lesovedenie* **2005**, *3*, 37–45. (In Russian)
61. Gorbach, N.; Startsev, V.; Mazur, A.; Milanovskiy, E.; Prokushkin, A.; Dymov, A. Simulation of Smoldering Combustion of Organic Horizons at Pine and Spruce Boreal Forests with Lab-Heating Experiments. *Sustainability* **2022**, *14*, 16772. [CrossRef]
62. Startsev, V.V.; Dymov, A.A.; Prokushkin, A.S. Soils of postpyrogenic larch stands in Central Siberia: Morphology, physicochemical properties, and specificity of soil organic matter. *Eurasian Soil Sci.* **2017**, *50*, 885–897. [CrossRef]
63. Sun, H.; Santalahti, M.; Pumpanen, J.; Köster, K.; Berninger, F.; Raffaello, T.; Jumpponen, A.; Asiegbu, F.O.; Heinonsalo, J. Fungal Community Shifts in Structure and Function across a Boreal Forest Fire Chronosequence. *Appl. Environ. Microbiol.* **2015**, *81*, 7869–7880. [CrossRef] [PubMed]
64. Köster, K.; Aaltonen, H.; Berninger, F.; Heinonsalo, J.; Köster, E.; Ribeiro-Kumara, C.; Sun, H.; Tedersoo, L.; Zhou, X.; Pumpanen, J. Impacts of wildfire on soil microbiome in Boreal environments. *Environ. Sci. Health* **2021**, *22*, 100258. [CrossRef]
65. Duchaufour, P.; Souchier, B. Roles of iron and clay in Genesis of acid soils under a humid, temperate climate. *Geoderma* **1978**, *20*, 15–26. [CrossRef]
66. Sapozhnikov, A.P.; Karpachevskii, L.O.; Il'ina, L.S. Postpyrogenic soil formation in Siberian pine—Broad leaved forests. *Lesn. Vestn.* **2001**, *1*, 132–164. (In Russian)

67. Wang, C.; Houlton, B.Z.; Liu, D.; Hou, J.; Cheng, W.; Bai, E. Stable isotopic constraints on global soil organic carbon turnover. *Biogeosciences* **2018**, *15*, 987–995. [CrossRef]
68. Lorenz, M.; Derrien, D.; Zeller, B.; Udelhoven, T.; Werner, W.; Thiele-Bruhn, S. The linkage of 13C and 15N soil depth gradients with C:N and O:C stoichiometry reveals tree species effects on organic matter turnover in soil. *Biogeochemistry* **2020**, *151*, 203–220. [CrossRef]
69. Angst, G.; Mueller, K.E.; Eissenstat, D.M.; Trumbore, S.; Freeman, K.; Hobbie, S.E.; Chorover, J.; Oleksyn, J.; Reich, P.B.; Mueller, C.W. Soil organic carbon stability in forests: Distinct effects of tree species identity and traits. *Glob. Chang. Biol.* **2018**, *25*, 1529–1546. [CrossRef]
70. Aaltonen, H.; Köster, K.; Köster, E.; Berninger, F.; Zhou, X.; Karhu, K.; Biasi, C.; Bruckman, V.; Palviainen, M.; Pumpanen, J. Forest fires in Canadian permafrost region: The combined effects of fire and permafrost dynamics on soil organic matter quality. *Biogeochemistry* **2019**, *143*, 257–274. [CrossRef]
71. Farquhar, G.D.; Ehleringer, J.R.; Hubick, K.T. Carbon isotope discrimination and photosynthesis. *Annu. Rev. Plant Physiol. Plant Mol. Biol.* **1989**, *40*, 503–537. [CrossRef]
72. Acton, P.; Fox, J.; Campbell, E.; Rowe, H.; Wilkinson, M. Carbon isotopes for estimating soil decomposition and physical mixing in well-drained forest soils. *J. Geophys. Res. Biogeosci.* **2013**, *118*, 1532–1545. [CrossRef]
73. Golubtsov, V.A. Stable Carbon Isotopic Composition of Organic Matter of the Late Pleistocene and Holocene Soils of the Baikal Region. *Eurasian Soil Sci.* **2020**, *53*, 724–738. [CrossRef]
74. Trumbore, S. Age of soil organic matter and soil respiration: Radiocarbon constraints on belowground C dynamics. *Ecol. Appl.* **2000**, *10*, 399–411. [CrossRef]
75. Stevenson, B.A.; Parfitt, R.L.; Schipper, L.A.; Baisden, W.T.; Mudge, P. Relationship between soil d15N, C/N and N losses across land uses in New Zealand Agriculture. *Ecosyst. Environ.* **2010**, *139*, 736–741. [CrossRef]
76. Liu, W.; Feng, X.; Ning, Y.; Zhang, Q.; Cao, Y.; Zhisheng, A.N. $\delta^{13}C$ variation of C3 and C4 plants across an Asian monsoon rainfall gradient in arid northwestern China. *Glob. Chang. Biol.* **2005**, *11*, 1094–1100. [CrossRef]
77. Wang, Z.; Liu, S.; Bu, Z.-J.; Wang, S. Degradation of polycyclic aromatic hydrocarbons (PAHs) during Sphagnum litters decay. *Environ. Sci. Pollut. Res.* **2018**, *25*, 18642–18650. [CrossRef]
78. Högberg, P. Tansley review No 95—N-15 natural abundance in soil-plant systems. *New Phytol.* **1997**, *137*, 179–203. [CrossRef] [PubMed]
79. Stevenson, B.; Kelly, E.; McDonald, E.; Busacca, A. The stable carbon isotope composition of soil organic carbon and pedogenic carbonates along a bioclimatic gradient in the Palouse region, Washington State, USA. *Geoderma* **2005**, *124*, 37–47. [CrossRef]
80. Boeckx, P.; Paulino, L.; Oyarzún, C.; van Cleemput, O.; Godoy, R. Soil δ15N patterns in old-growth forests of southern Chile as integrator for N-cycling. *Isot. Environ. Health Stud.* **2005**, *41*, 249–259. [CrossRef]
81. Natelhoffer, K.J.; Fry, B. Controls on Natural Nitrogen-15 and Carbon-13 Abundances in Forest Soil Organic Matter. *Soil Sci. Soc. Am. J.* **1988**, *52*, 1633–1640. [CrossRef]
82. Krull, E.S.; Skjemstad, J.O. $\delta^{13}C$ and $\delta^{15}N$ profiles in ^{14}C-dated Oxisol and Vertisols as a function of soil chemistry and mineralogy. *Geoderma* **2003**, *112*, 1–29. [CrossRef]
83. Jenkinson, D.; Coleman, K. The turnover of organic carbon in subsoils. Part 2. Modelling carbon turnover. *Eur. J. Soil Sci.* **2008**, *59*, 400–413. [CrossRef]
84. Nel, J.A.; Craine, J.M.; Cramer, M.D. Correspondence between δ13C and δ15N in soils suggests coordinated fractionation processes for soil C and N. *Plant Soil* **2017**, *423*, 257–271. [CrossRef]
85. Nave, L.E.; Vance, E.D.; Swanston, C.W.; Curtis, P.S. Fire effects on temperate forest soil C and N storage. *Ecol. Appl.* **2011**, *21*, 1189–1201. [CrossRef] [PubMed]
86. Larjavaara, M.; Berninger, F.; Palviainen, M.; Prokushkin, A.; Wallenius, T. Post-fire carbon and nitrogen accumulation and succession in Central Siberia. *Sci. Rep.* **2017**, *7*, 12776. [CrossRef]
87. Han, C.-L.; Sun, Z.-X.; Shao, S.; Wang, Q.-B.; Libohova, Z.; Owens, P.R. Changes of Soil Organic Carbon after Wildfire in a Boreal Forest, Northeast CHINA. *Agronomy* **2021**, *11*, 1925. [CrossRef]
88. Johnson, D.; Murphy, J.D.; Walker, R.F.; Glass, D.W.; Miller, W.W. Wildfire effects on forest carbon and nutrient budgets. *Ecol. Eng.* **2007**, *31*, 183–192. [CrossRef]
89. Palviainen, M.; Laurén, A.; Pumpanen, J.; Bergeron, Y.; Bond-Lamberty, B.; Larjavaara, M.; Kashian, D.M.; Köster, K.; Prokushkin, A.; Chen, H.Y.H.; et al. Decadal-scale recovery of carbon stocks after wildfires throughout the boreal forests. *Glob. Biogeochem. Cycles* **2020**, *34*, e2020GB006612. [CrossRef]
90. Kukavskaya, E.A.; Ivanova, G.A.; Conard, S.G.; McRae, D.J.; Ivanov, V.A. Biomass dynamics of central Siberian Scots pine forests following surface fires of varying severity. *Int. J. Wildland Fire* **2014**, *23*, 872–886. [CrossRef]
91. Walker, X.; Baltzer, J.L.; Cumming, S.G.; Day, N.J.; Ebert, C.; Goetz, S.; Johnstone, J.F.; Potter, S.; Rogers, B.M.; Schuur, E.A.G.; et al. Increasing wildfires threaten historic carbon sink of boreal forest soils. *Nature* **2019**, *572*, 520–523. [CrossRef] [PubMed]
92. Santín, C.; Doerr, S.H.; Preston, C.M.; González-Rodríguez, G. Pyrogenic organic matter production from wildfires: A missing sink in the global carbon cycle. *Glob. Chang. Biol.* **2015**, *21*, 1621–1633. [CrossRef] [PubMed]
93. Prokushkin, S.G.; Bogdanov, V.V.; Prokushkin, A.S.; Tokareva, I.V. Postpyrogenic restoration of vegetation in larch stands of the cryolithozone in Central Evenkia. *Biol. Bull.* **2011**, *38*, 183–190. [CrossRef]

94. Gonza'lez-Vila, F.J.; Gonza'lez, J.A.; Polvillo, O.; Almendros, G.; Knicker, H. Nature of refractory forms of organic carbon in soils affected by fires. Pyrolytic and spectroscopic approaches. In *Forest Fire Research and Wildland Fire Safety*; Viegas, D.X., Ed.; Millpress: Rotterdam, The Netherlands, 2002.
95. Knicker, H. How does fire affect the nature and stability of soil organic nitrogen and carbon? A review. *Biogeochemistry* **2007**, *85*, 91–118. [CrossRef]
96. Krasilnikov, P.V. Stable carbon compounds in soils: Their origin and functions. *Eurasian Soil Sci.* **2015**, *48*, 997–1008. [CrossRef]
97. Christensen, B.T. Physical fractionation of soil and structural and functional complexity in organic matter turnover. *Eur. J. Soil Sci.* **2001**, *52*, 345–353. [CrossRef]
98. Kögel-Knabner, I.; Amelung, W. Dynamics, Chemistry, and Preservation of Organic Matter in Soils. In *Treatise on Geochemistry*, 2nd ed.; Holland, H.D., Turekian, K.K., Eds.; Elsevier: Oxford, England, 2014; Volume 12, pp. 157–215.
99. Golchin, A.; Oades, J.; Skjemstad, J.; Clarke, P. Study of free and occluded particulate organic matter in soils by solid state 13C Cp/MAS NMR spectroscopy and scanning electron microscopy. *Soil Res.* **1994**, *32*, 285–309. [CrossRef]
100. Golchin, A.; Oades, J.M.; Skjemstad, J.O.; Clarke, P. Structural and dynamic properties of soil organic-matter as reflected by 13C natural-abundance, pyrolysis mass-spectrometry and solid-state 13C NMR-spectroscopy in density fractions of an oxisol under forest and pasture. *Soil Res.* **1995**, *33*, 59–76. [CrossRef]
101. Helfrich, M.; Ludwig, B.; Buurman, P.; Flessa, H. Effect of land use on the composition of soil organic matter in density and aggregate fractions as revealed by solid-state 13C NMR spectroscopy. *Geoderma* **2006**, *136*, 331–341. [CrossRef]
102. Wang, W.; Wang, Q.; Lu, Z. Soil organic carbon and nitrogen content of density fractions and effect of meadow degradation to soil carbon and nitrogen of fractions in alpine Kobresia meadow. *Sci. China Ser. D Earth Sci.* **2009**, *52*, 660–668. [CrossRef]
103. Guareschi, R.F.; Pereira, M.G.; Perin, A. Densimetric fractionation of organic matter in an agricultural chronosequence in no-till areas in the Cerrado region, Brazil. *Semin. Ciências Agrárias* **2016**, *37*, 595–610. [CrossRef]
104. Startsev, V.; Khaydapova, D.; Degteva, S.; Dymov, A. Soils on the southern border of the cryolithozone of European part of Russia (the Subpolar Urals) and their soil organic matter fractions and rheological behavior. *Geoderma* **2019**, *361*, 114006. [CrossRef]
105. Lehmann, J.; Gaunt, J.; Rondon, M.B. Bio-char Sequestration in Terrestrial Ecosystems—A Review. *Mitig. Adapt. Strat. Glob. Change* **2006**, *11*, 403–427. [CrossRef]
106. Startsev, V.V.; Yakovleva, E.V.; Kutyavin, I.N.; Dymov, A.A. Fire Impact on Carbon Pools and Basic Properties of Retisols in Native Spruce Forests of the European North and Central Siberia of Russia. *Forests* **2022**, *13*, 1135. [CrossRef]
107. Schmidt, M.W.I.; Noack, A.G. Black carbon in soils and sediments: Analysis, distribution, implications, and current challenges. *Glob. Biogeochem. Cycles* **2000**, *14*, 777–793. [CrossRef]
108. Preston, C.M.; Schmidt, M.W.I. Black (pyrogenic) carbon: A synthesis of current knowledge and uncertainties with special consideration of boreal regions. *Biogeosciences* **2006**, *3*, 397–420. [CrossRef]
109. Czimczik, C.I.; Masiello, C. Controls on black carbon storage in soils. *Glob. Biogeochem. Cycles* **2007**, *21*, GB3005. [CrossRef]
110. Masiello, C. New directions in black carbon organic geochemistry. *Mar. Chem.* **2004**, *92*, 201–213. [CrossRef]
111. Hockaday, W.C.; Grannas, A.M.; Kim, S.; Hatcher, P.G. Direct molecular evidence for the degradation and mobility of black carbon in soils from ultrahigh-resolution mass spectral analysis of dissolved organic matter from a fire-impacted forest soil. *Org. Geochem.* **2006**, *37*, 501–510. [CrossRef]
112. García-Falcón, M.S.; Soto-González, B.; Simal-Gándara, J. Evolution of the 15 Concentrations of Polycyclic Aromatic Hydrocarbons in Burnt Woodland Soils. *Environ. Sci. Technol.* **2006**, *40*, 759–763. [CrossRef]
113. Campos, I.; Abrantes, N.; Pereira, P.; Micaelo, A.C.; Vale, C.; Keizer, J.J. Forest fires as potential triggers for production and mobilization of polycyclic aromatic hydrocarbons to the terrestrial ecosystem. *Land Degrad. Dev.* **2019**, *30*, 2360–2370. [CrossRef]
114. Chen, R.; Lv, J.; Zhang, W.; Liu, S.; Feng, J. Polycyclic aromatic hydrocarbon (PAH) pollution in agricultural soil in Tianjin, China: A spatio-temporal comparison study. *Environ. Earth Sci.* **2015**, *74*, 2743–2748. [CrossRef]
115. Vasconcelos, U.; de França, F.P.; Oliveira, F.J.S. Removal of high-molecular weight polycyclic aromatic hydrocarbons. *Química Nova* **2011**, *34*, 218–221. [CrossRef]
116. Sihi, D.; Inglett, P.W.; Inglett, K.S. Warming rate drives microbial nutrient demand and enzyme expression during peat decomposition. *Geoderma* **2018**, *336*, 12–21. [CrossRef]
117. Nemirovskaya, I.A. Hydrocarbons in the White Sea: Routes and forms of migration and genesis. *Geochem. Int.* **2005**, *43*, 493–504.
118. Gabov, D.N.; Beznosikov, V.A.; Kondratenok, B.M. Polycyclic aromatic hydrocarbons in background podzolic and gleyic peat-podzolic soils. *Eurasian Soil Sci.* **2007**, *40*, 256–264. [CrossRef]
119. Lu, G.-N.; Danga, Z.; Tao, X.-Q.; Yanga, C.; Yi, X.-Y. Estimation of Water Solubility of Polycyclic Aromatic Hydrocarbons Using Quantum Chemical Descriptors and Partial Least Squares. *QSAR Comb. Sci.* **2008**, *27*, 618–626. [CrossRef]
120. Gabov, D.N.; Beznosikov, V.A. Polycyclic aromatic hydrocarbons in tundra soils of the Komi Republic. *Eurasian Soil Sci.* **2014**, *47*, 18–25. [CrossRef]
121. García, R.; Diaz-Somoano, M.; Calvo, M.; López-Antón, M.A.; Suárez, S.; Ruiz, I.S.; Martínez-Tarazona, M.R. Impact of a semi-industrial coke processing plant in the surrounding surface soil. Part II: PAH content. *Fuel Process. Technol.* **2012**, *104*, 245–252. [CrossRef]